

Light front synchronization and rest frame densities of the proton: I. Electromagnetic densities

Adam Freese^{1,*} and Gerald A. Miller^{1,†}

¹*Department of Physics, University of Washington, Seattle, WA 98195, USA*

We clarify the physical origin and meaning of the two-dimensional relativistic densities of the light front formalism. The densities are shown to originate entirely from the use of light front time instead of instant form time, which physically corresponds to using an alternative synchronization convention. This is shown by using tilted light front coordinates, which consist of light front time and ordinary spatial coordinates, and which are also used to show that the obtained densities describe a system at rest rather than at infinite momentum. These coordinates allow all four components of the electromagnetic current density to be given clear physical meanings. We explicate the formalism for spin-half targets, obtaining charge and current densities of the proton and neutron using empirical form factor parametrizations, as well as up and down quark densities and currents. Angular modulations in the densities of transversely-polarized states are explained as originating from redshifts and blueshifts due to quarks moving in different longitudinal directions.

I. INTRODUCTION

There has recently been renewed interest and debate about the proper manner of understanding spatial densities of hadrons, especially regarding their application to the energy-momentum tensor [1–4]. This interest is especially pertinent to the upcoming Electron Ion Collider [5–7], since spatial tomography of partons in hadrons is one of the facility’s central focuses. It is vital to the success of this program that an accurate formalism be employed to obtain spatial distributions of partons within hadrons.

For the longest time, most authors have calculated relativistic densities using three-dimensional Fourier transforms of form factors, obtaining results referred to as Breit frame densities or Sachs densities [8]. For a long time, too, this approach has been criticized as relativistically inexact and as not following from elementary field-theoretic definitions [9–11]. While most authors continue to use Breit frame densities uncritically, a variety of criticisms and defenses of the Breit frame densities and alternative formalisms have been proposed (see Refs. [2, 9–15] for a variety of perspectives).

The light front formalism has stood out in these debates as providing relativistically exact two-dimensional densities [16, 17] that can be obtained from elementary field-theoretic definitions [3, 10] in a wave-packet-independent way [15]. Additionally, the light front densities are related to generalized parton distributions [11, 16, 18], which simultaneously encode electromagnetic and gravitational form factors through their polynomiality property [19, 20], and which extend light front densities to three-dimensional distributions over the transverse plane and the light front momentum fraction x .

Despite the success of the light front formalism, misgivings about light front densities persist. It is widely believed that light front densities describe the apparent structure of a system moving at the speed of light, and thus contain kinematic distortions caused by boosting to infinite momentum. Another criticism—given in Ref. [14] for instance—is that the “minus” components of four-vector and tensor densities do not have clear meanings, and indeed existing works on light front densities merely ignore these components.

Both of these misgivings can be addressed with a minor change to the light front coordinates. By using light front time $x^+ = t + z$ with ordinary spatial coordinates (x, y, z) —an idea first explored in Ref. [21], where these are called *tilted light front coordinates*—all existing results for light front densities are reproduced, but the previously-neglected components of vectors and tensors obtain clear physical meanings. Moreover, by using ordinary spatial coordinates, it can unambiguously be shown that the previously-known and newly-found light front densities alike describe a system moving at any velocity, even a system at rest.

The use of tilted light front coordinates has a straightforward conceptual interpretation: using light front time x^+ instead of instant form time t simply means changing the rules for how spatially distant clocks are synchronized. In this work, we will show how the entire formalism of light front densities follows from changing the time synchronization convention. Due to the lengthy exposition required for the coordinate system, this paper will focus entirely on electromagnetic densities of spin-half systems; the energy-momentum tensor will be explored in a sequel work.

This work is organized as follows. Tilted coordinates are defined in Sec. II, which also contains a detailed exposition of their properties: general properties are explored in Sec. II A; Lorentz transforms in Sec. II B; conserved currents and identification of the “charge” component in Sec. II C. The wave packet and spin density matrix are constructed in Sec. III. The formulas for intrinsic electromagnetic densities of spin-half systems are derived in Sec. IV. In Sec. V, these formulas are applied to empirical proton and neutron form factors to obtain charge and current densities, as well as up and down quark densities. We provide concluding remarks and an outlook in Sec. VI. A uniqueness proof for light front synchronization is given in Appendix B.

* afreese@uw.edu

† miller@uw.edu

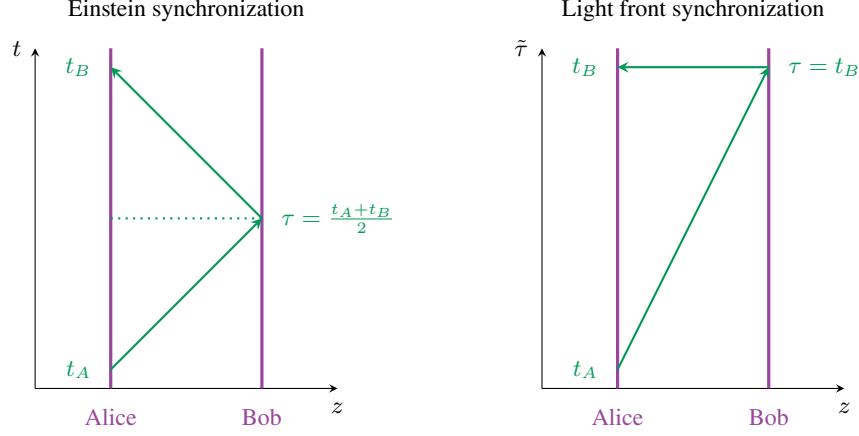


FIG. 1. Pictorial representations of time synchronization conventions. In these pictures, Alice sends a light signal to Bob, who promptly sends a return signal. The time $\Delta t = t_B - t_A$ elapsed throughout the exchange from Alice’s perspective is a local observable, independent of synchronization convention. In the Einstein convention (left panel), the local time measured by Bob’s clock when the signal is reflected is halfway between the start and end times. In light front synchronization (right panel), the clocks are synchronized under the convention that the return signal travels instantaneously, so Bob’s clock reads t_B when the signal is reflected. The invariance of Δt requires that the signal to Bob travel at $c/2$ in this convention.

II. TILTED COORDINATES AND LIGHT FRONT SYNCHRONIZATION

Tilted light front coordinates (hereafter “tilted coordinates”) were first defined by Blunden, Burkardt and Miller (BBM) in Ref. [21]¹:

$$\tilde{\tau} = \tilde{x}^0 \equiv x^+ = t + z \quad (1a)$$

$$\tilde{x}^1 \equiv x \quad (1b)$$

$$\tilde{x}^2 \equiv y \quad (1c)$$

$$\tilde{x}^3 \equiv z. \quad (1d)$$

We use tildes for quantities in tilted coordinates for clarity. The three spatial coordinates are the usual Cartesian coordinates of Euclidean space. Crucially, this means that a system at rest in tilted coordinates is really at rest as understood by common sense.

The tilted time variable $\tilde{\tau}$ is the same as light front time, and can be given an operational meaning. In fact, the familiar time t of Minkowski coordinates is also defined operationally, as first clarified by Einstein [22]. The local time τ at which an event occurs is determined by its simultaneity with the reading of a clock in the local vicinity of the event. Einstein postulates *by definition* (“*durch Definition*”—his emphasis) that distant clocks be synchronized by light signals under the convention that the time delay of the signal is equal in both directions. This definition has come to be called the Einstein synchronization convention, and using it gives us the Einstein (or instant form) time coordinate $\tau = x^0 = t$. A pictorial representation of this convention is given in the left panel of Fig. 1.

The use of Einstein’s convention is ultimately arbitrary—a point which has been discussed for a long time by both physicists (see Refs. [23, 24] and references therein) and philosophers [25, 26]². The use of an anisotropic synchronization convention notoriously results in the same empirical predictions as Einstein’s convention, since mathematically this merely corresponds to a coordinate transformation [24].

Light front time (and thus tilted time) is defined using an anisotropic synchronization convention, which we call light front synchronization. Observers aligned in the z direction synchronize their clocks *under the convention that* light travels instantaneously in the $-z$ direction. For instance, if Alice is located downstream of Bob ($z_{\text{Alice}} < z_{\text{Bob}}$), she synchronizes her clock to read the time she currently sees on Bob’s clock. This is depicted in the right panel of Fig. 1. The local time elapsed during the signal’s round trip is convention-independent, meaning the two-way speed of light is given by the invariant constant c [23, 25]. Under light front synchronization, this means light must travel at $c/2$ in the $+z$ direction, as depicted in the right panel of Fig. 1. Clocks at the same z coordinate but displaced in the transverse xy plane are synchronized using the Einstein convention. Following these rules for clock synchronization gives us the light front time $\tau = \tilde{x}^0 = x^+$.

¹ BBM use $\zeta = -z$ instead of $\tilde{z} = z$ as a coordinate, but this is a minor difference.

² This feature of special relativity has also recently been popularized by the science education channel Veritasium [27].

As noted above, the empirical predictions of a relativistic theory are independent of the synchronization convention. The use of a particular convention is ultimately arbitrary, but different conventions may be more conducive to solving particular problems. The motivation for using light front synchronization—and thus tilted coordinates—is that light front time is invariant under a Galilean subgroup of the Poincaré group [16, 28]. Ultimately, this allows physical densities at fixed $\tilde{\tau}$ to be separated into state-independent internal structures and state-dependent smearing functions in the manner explored in Ref. [15].

A. Properties of tilted coordinates

Let us consider some of the properties of tilted coordinates, especially since they differ from the more familiar light front coordinates. Some of these properties were reported previously by BBM [21], but some of these relationships are new. Firstly, the metric and inverse metric are given by:

$$\tilde{g}_{\mu\nu} = \frac{\partial x^\alpha}{\partial \tilde{x}^\mu} \frac{\partial x^\beta}{\partial \tilde{x}^\nu} g_{\alpha\beta} = \begin{bmatrix} 1 & 0 & 0 & -1 \\ 0 & -1 & 0 & 0 \\ 0 & 0 & -1 & 0 \\ -1 & 0 & 0 & 0 \end{bmatrix} \quad (2a)$$

$$\tilde{g}^{\mu\nu} = \frac{\partial \tilde{x}^\mu}{\partial x^\alpha} \frac{\partial \tilde{x}^\nu}{\partial x^\beta} g^{\alpha\beta} = \begin{bmatrix} 0 & 0 & 0 & -1 \\ 0 & -1 & 0 & 0 \\ 0 & 0 & -1 & 0 \\ -1 & 0 & 0 & -1 \end{bmatrix} \quad (2b)$$

where $g_{\mu\nu} = g^{\mu\nu} = \text{diag}(+1, -1, -1, -1)$ is the usual Minkowski metric³. This means that the invariant proper time element is given by:

$$ds^2 = \tilde{g}_{\mu\nu} d\tilde{x}^\mu d\tilde{x}^\nu = d\tilde{\tau}^2 - 2 d\tilde{\tau} d\tilde{z} - d\tilde{x}_\perp^2, \quad (3)$$

where $\tilde{x}_\perp = (\tilde{x}, \tilde{y})$ are the transverse coordinates, while the d'Alembertian is given by:

$$\partial^2 = \tilde{g}^{\mu\nu} \tilde{\partial}_\mu \tilde{\partial}_\nu = -2\tilde{\partial}_z \tilde{\partial}_\tau - \tilde{\nabla}^2, \quad (4)$$

where $\tilde{\nabla} = (\tilde{\partial}_x, \tilde{\partial}_y, \tilde{\partial}_z)$ is the three-dimensional gradient. The latter was found previously by BBM [21].

Covariant components of a four-vector \tilde{A}_μ (lower index) are related to contravariant components \tilde{A}^μ (upper index) through the metric:

$$\tilde{A}_\mu = \tilde{g}_{\mu\nu} \tilde{A}^\nu \quad \tilde{A}^\mu = \tilde{g}^{\mu\nu} \tilde{A}_\nu, \quad (5a)$$

which in terms of individual components gives:

$$\tilde{A}_0 = \tilde{A}^0 - \tilde{A}^3 \quad \tilde{A}^0 = -\tilde{A}_3 \quad (5b)$$

$$\tilde{A}_1 = -\tilde{A}^1 \quad \tilde{A}^1 = -\tilde{A}_1 \quad (5c)$$

$$\tilde{A}_2 = -\tilde{A}^2 \quad \tilde{A}^2 = -\tilde{A}_2 \quad (5d)$$

$$\tilde{A}_3 = -\tilde{A}^0 \quad \tilde{A}^3 = -\tilde{A}_0 - \tilde{A}_3. \quad (5e)$$

Components of four-momentum are defined as generators of spacetime translations:

$$i[\hat{P}_\mu, \hat{O}(x)] = \partial_\mu \hat{O}(x), \quad (6)$$

and accordingly the energy and vector momentum are identified using the covariant vector \tilde{p}_μ :

$$\tilde{p}_\mu \equiv (\tilde{E}; -\tilde{p}_x, -\tilde{p}_y, -\tilde{p}_z). \quad (7)$$

Note that when we use x , y or z as a subscript, we are indicating a component of the three-vector $\tilde{\mathbf{p}}$ rather than components of the four-vector p_μ :

$$\tilde{\mathbf{p}} = (\tilde{p}_x, \tilde{p}_y, \tilde{p}_z) = (-\tilde{p}_1, -\tilde{p}_2, -\tilde{p}_3). \quad (8)$$

³ Note that, while using tilted coordinates, we use numerical indices 0, 1, 2, 3 rather than +, 1, 2, 3 to label components of tensors.

With this identification, the tilted energy and vector momentum become time and space translation generators as usual:

$$i[\tilde{E}, \hat{O}(x)] = \tilde{\partial}_0 \hat{O}(x) \quad (9a)$$

$$-i[\tilde{\mathbf{p}}, \hat{O}(x)] = \tilde{\nabla} \hat{O}(x). \quad (9b)$$

The scalar product between four-momentum and a spacetime coordinate is:

$$\tilde{p} \cdot \tilde{x} = \tilde{p}_\mu \tilde{x}^\mu = \tilde{E} \tilde{\tau} - \tilde{\mathbf{p}} \cdot \tilde{\mathbf{x}}, \quad (10)$$

which is a point of central importance to the density formalism. The mass-shell relation can be written:

$$m^2 = \tilde{g}^{\mu\nu} \tilde{p}_\mu \tilde{p}_\nu = 2\tilde{p}_z \tilde{E} - \tilde{\mathbf{p}}^2 \quad (11a)$$

$$\tilde{E} = \frac{m^2 + \tilde{\mathbf{p}}^2}{2\tilde{p}_z}, \quad (11b)$$

which was found previously by BBM [21].

The relationships between the tilted and Minkowski four-momenta can be found using:

$$\tilde{p}_\mu = \frac{\partial x^\nu}{\partial \tilde{x}^\mu} p_\nu, \quad (12)$$

which entails:

$$\tilde{E} = E \quad (13a)$$

$$\tilde{p}_x = p_x \quad (13b)$$

$$\tilde{p}_y = p_y \quad (13c)$$

$$\tilde{p}_z = E + p_z = p^+. \quad (13d)$$

Two remarkable things have happened here. Firstly, the tilted energy is equal to the instant form energy. This means that a mass decomposition in tilted coordinates will be the same as a mass decomposition in Minkowski coordinates (in contrast to the standard light front energy p^- [29]), and a spatial density of \tilde{E} is a density of the familiar instant form energy E . Secondly, the conjugate momentum to the z coordinate is p^+ , which is the momentum variable used to define momentum fractions in parton distribution functions and generalized parton distributions. This suggests that the formalism for PDFs and GPDs can be translated into tilted coordinates, and thus also understood in terms of light front synchronization rather than an infinite-momentum frame.

Lastly, we discuss particle velocities and the conditions for a particle being at rest. Classically, the velocity of a free particle is obtained from Hamilton's equations:

$$\tilde{v}_a = \frac{\partial \tilde{E}}{\partial \tilde{p}_a}, \quad (14a)$$

(where $a = x, y, z$) which, upon using Eq. (11b) gives

$$\tilde{v}_x = \frac{\tilde{p}_x}{\tilde{p}_z} \quad (14b)$$

$$\tilde{v}_y = \frac{\tilde{p}_y}{\tilde{p}_z} \quad (14c)$$

$$\tilde{v}_z = 1 - \frac{\tilde{E}}{\tilde{p}_z} \quad (14d)$$

for the individual components of the velocity. All three of these can be summarized with the help of Eq. (5) as:

$$\tilde{v}^i = \frac{\tilde{p}^i}{\tilde{p}_z}. \quad (14e)$$

Note the upper index in the components of the momentum four-vector here. This relationship can be made quantum mechanical simply by promoting it to an operator relationship. The free particle is at rest when $\tilde{\mathbf{v}} = 0$, which occurs when:

$$\tilde{p}_x = 0 \quad (15a)$$

$$\tilde{p}_y = 0 \quad (15b)$$

$$\tilde{p}_z = m. \quad (15c)$$

The relationship between longitudinal velocity and longitudinal momentum is strange and counter-intuitive, but follows from the elementary definition of momentum as the generator of spatial translations *at a fixed time* (which is fixed light front time here). Regardless, Eq. (15) allows us to clearly identify if a particle is at rest—and since the spatial coordinates $\tilde{\mathbf{x}} = \mathbf{x}$ are the usual Cartesian coordinates, a system at rest with respect to these coordinates is unambiguously at rest as understood by common sense.

B. Lorentz transforms and the Galilean subgroup

We next explore the algebra of the Lorentz group and the effects of finite boosts in tilted coordinates. Since the goal of this work is to obtain rest frame densities, special focus will be given to properties that are invariant under boosts, since these properties remain unaltered when boosting the system to rest.

The standard generator basis for the Poincaré group in Minkowski coordinates consists of four translation generators P_μ and six Lorentz transform generators $J^{\mu\nu} = -J^{\nu\mu}$, with the latter consisting of three rotation generators $\mathbf{J} = (J^{23}, J^{31}, J^{12})$ and three boost generators $\mathbf{K} = (J^{10}, J^{20}, J^{30})$. We have already discussed the translation generators in tilted coordinates above. The tilted rotation generators are the same as in instant form coordinates, $\tilde{\mathbf{J}} = \mathbf{J}$, since the same spatial coordinates are used in both systems. The boosts in tilted coordinates remain to be analyzed.

Under an *infinitesimal* passive transverse *instant form* boost, with velocities $d\beta_x$ and $d\beta_y$ in the x and y directions, the instant form coordinates transform as:

$$t' = t - d\beta_x x - d\beta_y y \quad (16a)$$

$$x' = x - d\beta_x t \quad (16b)$$

$$y' = y - d\beta_y t \quad (16c)$$

$$z' = z. \quad (16d)$$

In terms of tilted coordinates, this same infinitesimal transformation can be written:

$$\tilde{\tau}' = \tilde{\tau} - d\beta_x \tilde{x} - d\beta_y \tilde{y} \quad (17a)$$

$$\tilde{x}' = \tilde{x} - d\beta_x \tilde{\tau} + d\beta_x \tilde{z} \quad (17b)$$

$$\tilde{y}' = \tilde{y} - d\beta_y \tilde{\tau} + d\beta_y \tilde{z} \quad (17c)$$

$$\tilde{z}' = \tilde{z}. \quad (17d)$$

Remarkably, this transformation is not merely a boost in tilted coordinates, but a combined boost and rotation. In fact, this is the origin of Terrell-Penrose rotations [30, 31]: what is merely boost according to a spatially extended reference frame with clocks synchronized by the Einstein convention *looks like* a boost and a rotation, and in fact *is* a boost and a rotation under the light front synchronization convention. Because of this, to define a mere boost in tilted coordinates, we must counteract the Terrell-Penrose rotation. The appropriate boost generators are:

$$\tilde{B}_1 = K_1 - J_2 \quad (18a)$$

$$\tilde{B}_2 = K_2 + J_1. \quad (18b)$$

The remaining boost generator remains unmodified:

$$\tilde{B}_3 = K_3. \quad (18c)$$

All three of these boosts modify the \tilde{z} coordinate in unintuitive ways. Under a finite *light front* transverse boost by a velocity v along the x direction, the tilted coordinates transform as:

$$\tilde{\tau}' = \tilde{\tau} \quad (19a)$$

$$\tilde{x}' = \tilde{x} - v\tilde{\tau} \quad (19b)$$

$$\tilde{y}' = \tilde{y} \quad (19c)$$

$$\tilde{z}' = \tilde{z} + v\tilde{x} - \frac{v^2}{2}\tilde{\tau}, \quad (19d)$$

while under a finite longitudinal boost of rapidity⁴ η they transform as:

$$\tilde{\tau}' = e^{-\eta}\tilde{\tau} \quad (20a)$$

$$\tilde{x}' = \tilde{x} \quad (20b)$$

$$\tilde{y}' = \tilde{y} \quad (20c)$$

$$\tilde{z}' = e^\eta\tilde{z} - \sinh(\eta)\tilde{\tau}. \quad (20d)$$

⁴ Recall that in instant form coordinates, the rapidity of a boost is given by $\eta = \frac{1}{2} \log \left(\frac{c+v_{\text{IF}}}{c-v_{\text{IF}}} \right)$. In tilted coordinates, Eq. (21) instead gives the relationship between rapidity and longitudinal velocity.

An object that is stationary in the original frame moves with a velocity

$$v_z = -e^\eta \sinh(\eta) = \frac{1}{2}(1 - e^{2\eta}) \quad (21)$$

in the new frame, which is bounded to $(-\infty, 1/2)$ —the bounds being the one-way speed of light in each direction along the z axis.

The longitudinal boost is worth understanding conceptually. Let $\Delta\tilde{\tau}$ be a time interval measured by a clock in the original frame; the same time interval according to the transformed frame will be $\Delta\tilde{\tau}' = e^{-\eta}\Delta\tilde{\tau}$. Since the boost was a passive transformation, the now-moving clock will measure the interval $\Delta\tilde{\tau} = e^\eta\Delta\tilde{\tau}'$ while a stationary clock in the new frame measures $\Delta\tilde{\tau}'$. Thus, when $\eta > 0$, time measured by the moving clock is dilated, while it is instead quickened when $\eta < 0$.

Next, let $\Delta\tilde{z}$ be the length between two comoving bodies as measured in the original frame; the length will be $\Delta\tilde{z}' = e^\eta\Delta\tilde{z}$ in the transformed frame. If $\eta > 0$, the length will appear dilated to the observer in the new frame, while when $\eta < 0$ the length appears contracted.

These transformation properties make sense when we recall the meaning behind light front synchronization discussed in Sec. II. To an observer downstream of (with a lesser \tilde{z} coordinate than) the system under observation, $\eta > 0$ means the system is moving away from the observer (in the $+z$ direction), and $\eta < 0$ means the system is moving towards them. For $\eta > 0$, the dilation of time and length of a moving system corresponds to a redshift while the time quickening and length contraction of a system moving with $\eta < 0$ corresponds to a blueshift. These are exactly the usual relativistic redshift and blueshift.

The Poincaré group has long been known to have a $(2+1)$ -dimensional Galilean subgroup [16, 28, 32–34]. This subgroup is generated by the basis $\{\tilde{E}, \tilde{P}_\perp^i, \tilde{P}_z, \tilde{J}_3, \tilde{B}_\perp^i\}$, where the \perp subscript means i only runs over 1 and 2. Under this group, the time $\tilde{\tau}$ remains invariant. The algebra of this subgroup is:

$$[\tilde{J}_3, \tilde{B}_\perp^i] = i\epsilon_{ij3}\tilde{B}_\perp^j \quad (22a)$$

$$[\tilde{B}_\perp^i, \tilde{B}_\perp^j] = 0 \quad (22b)$$

$$[\tilde{J}_3, \tilde{P}_\perp^i] = i\epsilon_{ij3}\tilde{P}_\perp^j \quad (22c)$$

$$[\tilde{B}_\perp^i, \tilde{P}_\perp^j] = i\delta_{ij}\tilde{P}_z \quad (22d)$$

$$[\tilde{B}_\perp^i, \tilde{E}] = i\tilde{P}_\perp^i, \quad (22e)$$

with all other commutators zero. Notably, \tilde{P}_z commutes with all other generators in the group. It is accordingly considered a central charge of the group, and this observation is identical to the well-known fact that P^+ is a central charge of the Galilean subgroup in light front coordinates [16, 28]. Physically, this means that the transformations in the Galilean subgroup (including all translations, transverse boosts, and rotations around the z axis) will leave \tilde{P}_z unaltered.

The Galilean subgroup has another central charge, which is related to the Pauli-Lubanski axial four-vector [35, 36]:

$$W_\mu = -\frac{1}{2}\epsilon_{\mu\nu\rho\sigma}J^{\nu\rho}P^\sigma, \quad (23)$$

defined with the convention that $\epsilon^{0123} = +1$. For its expression in tilted coordinates, one need only put tildes over each of the tensors involved. Just as with momentum, we define individual components of the associated three-vector using the covariant components of the Pauli-Lubanski vector: $\tilde{W}_\mu = (\tilde{W}_0; -\tilde{W}_x, -\tilde{W}_y, -\tilde{W}_z)$. Through some algebra, one can show that:

$$\tilde{W}_z = \tilde{P}_z\tilde{J}_3 - (\tilde{\mathbf{B}}_\perp \times \tilde{\mathbf{P}}_\perp) \cdot \hat{z}, \quad (24)$$

and additionally one can show that \tilde{W}_z commutes with all the generators of the Galilean subgroup, making it another central charge of this group. Additionally,

$$\hat{\lambda} = \tilde{P}_z^{-1}\tilde{W}_z = \tilde{J}_3 - \tilde{P}_z^{-1}(\tilde{\mathbf{B}}_\perp \times \tilde{\mathbf{P}}_\perp) \cdot \hat{z} \quad (25)$$

is invariant under the Galilean subgroup, and is equal to the z component of angular momentum for a system at transverse rest. The operator $\hat{\lambda}$ is the standard light front helicity operator [28], and characterizes the z component of intrinsic spin in a Galilean-invariant manner. Note that while light front helicity was originally conceived as an observable that becomes ordinary helicity in the infinite-momentum limit [28], we have found that it also coincides at rest to the spin projection along the z axis.

One can show that, under longitudinal boosts:

$$[\tilde{B}_3, \tilde{P}_z] = i\tilde{P}_z \quad (26a)$$

$$[\tilde{B}_3, \tilde{W}_z] = i\tilde{W}_z \quad (26b)$$

$$[\tilde{B}_3, \hat{\lambda}] = 0. \quad (26c)$$

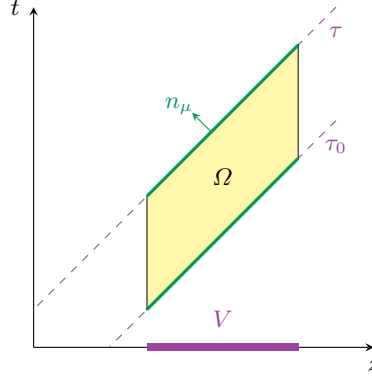


FIG. 2. A finite spacetime region Ω bounded by two hypersurfaces of equal light front time τ_0 and τ . Each slice of fixed light front time contains the same spatial region V . The future-directed normal n_μ to the equal-light-front-time hypersurfaces is also indicated in this diagram.

The light front helicity operator $\hat{\lambda}$ is invariant under longitudinal boosts. This makes light front helicity an especially useful label for characterizing the spin states of hadrons: a rest frame state with definite λ can be transformed to an arbitrary momentum state with the same λ by performing a longitudinal boost followed by a transverse boost. We will therefore use light front helicity to label the spin content of hadrons throughout the remainder of this work.

C. Conserved currents and densities at fixed light front time

Before proceeding to the construction of internal hadronic densities, it is important to understand how conserved currents should be understood in terms of light front time, especially for correctly identifying which component should be identified as the static density (e.g., as the charge density or as the energy density). A conserved current obeys the differential continuity equation:

$$\partial_\mu j^\mu(x) = \tilde{\partial}_\mu \tilde{j}^\mu(x) = 0, \quad (27)$$

which is the same in Minkowski and tilted coordinates. We will first proceed using Minkowski coordinates. The continuity equation can be cast into integral form by integrating it over a spacetime region Ω :

$$\int_\Omega d^4x \partial_\mu j^\mu(x) = 0. \quad (28)$$

The specific region of spacetime considered consists of a spatial volume V bounded by two equal-light-front-time hypersurfaces at $x^+ = \tau_0$ and $x^+ = \tau$, and is depicted in Fig. 2. Using the divergence theorem, the integral of the continuity equation over Ω can be rewritten as an integral over its surface. If we take n_μ to be the future-pointing normal vector to the equal-light-front-time surfaces, then:

$$\int_V d^3\mathbf{x} n_\mu j^\mu(x) \Big|_{x^+=\tau} - \int_V d^3\mathbf{x} n_\mu j^\mu(x) \Big|_{x^+=\tau_0} + \int_{\tau_0}^{\tau} d\tau' \int_{\partial V} d\mathbf{S} \cdot \mathbf{j}(x) \Big|_{x^+=\tau'} = 0, \quad (29)$$

and then differentiating this with respect to τ gives:

$$\frac{d}{d\tau} \left[\int_V d^3\mathbf{x} n_\mu j^\mu(x) \Big|_{x^+=\tau} \right] = - \int_{\partial V} d\mathbf{S} \cdot \mathbf{j}(x) \Big|_{x^+=\tau}. \quad (30)$$

This form has a clear interpretation as the integral form of a continuity equation. The left-hand side quantifies how the amount of “charge” in a spatial region V is changing with time, and the right-hand side quantifies how much current is flowing through the boundary of this spatial region at a fixed light front time τ . The right-hand side becomes zero if V is all of space and j^μ is localized in space (as is expected of physically realistic currents), and in this case the equation is just a statement of charge conservation. Since this relation must hold for any spatial region V , the static charge density is given by

$$\rho(x) = n_\mu j^\mu(x) = j^+(x) \quad (31)$$

when expressed in Minkowski coordinates, which is identical to the standard light front charge density. This is the logical result of using light front time synchronization, and not an arbitrary choice.

The same derivation can be done using tilted instead of Minkowski coordinates. Fixed-time surfaces are given by fixed $\tilde{\tau}$, and the future-pointing normal to equal light front time surfaces gives

$$\rho(x) = \tilde{n}_\mu \tilde{j}^\mu(x) = \tilde{j}^0(x). \quad (32)$$

Comparing to Eq. (1), one can see that $\tilde{j}^0(x) = j^+(x)$, so these coordinate systems give consistent results if the same equal-light-front-time surface is used in both. The vector current is given by $\tilde{\mathbf{j}}(x) = \mathbf{j}(x)$ regardless of synchronization convention.

III. WAVE PACKETS AND PROBABILITY CURRENTS IN TILTED COORDINATES

To isolate purely internal properties of composite spin-half systems, we require a formulation for the wave function describing the location of the system itself. We shall construct that formulation here, along with four-currents for the probability and spin projections, which will appear in Sec. IV as smearing functions.

We assume that it is possible to prepare a state with a single particle of the species under consideration; we consider a proton for concreteness. Single-proton states are characterized by the three independent components of their four-momentum, namely $\tilde{\mathbf{p}}$, as well as their light front helicity λ . As noted by BBM [21], light front quantization can be used with tilted coordinates, since equal-time surfaces are defined the same way in both systems. The creation and annihilation operators for the proton field obey the canonical anticommutation relations:

$$\{b(\tilde{\mathbf{p}}, \lambda), b^\dagger(\tilde{\mathbf{p}}', \lambda')\} = \{d(\tilde{\mathbf{p}}, \lambda), d^\dagger(\tilde{\mathbf{p}}', \lambda')\} = 2\tilde{p}_z (2\pi)^3 \delta^{(3)}(\tilde{\mathbf{p}} - \tilde{\mathbf{p}}') \delta_{\lambda\lambda'}, \quad (33)$$

and all other anticommutators are zero. Here, b and b^\dagger annihilate and create protons, while d and d^\dagger annihilate and create anti-protons. Single-proton states of definite momentum are given by:

$$|\tilde{\mathbf{p}}, \lambda\rangle = b^\dagger(\tilde{\mathbf{p}}, \lambda)|0\rangle, \quad (34)$$

and the projection operator for identifying single-proton states is:

$$A_{1p} = \sum_\lambda \int \frac{d^3\tilde{\mathbf{p}}}{2\tilde{p}_z (2\pi)^3} |\tilde{\mathbf{p}}, \lambda\rangle \langle \tilde{\mathbf{p}}, \lambda|. \quad (35)$$

Let $|\Psi\rangle$ signify a normalized single-proton state, meaning:

$$\langle\Psi|\Psi\rangle = 1 \quad (36a)$$

$$|\Psi\rangle = A_{1p}|\Psi\rangle. \quad (36b)$$

When dealing with such a state, we can treat A_{1p} as an identity operator and use Eq. (35) as a completeness relation. The momentum-representation wave function can be defined as $\langle\tilde{\mathbf{p}}, \lambda|\Psi\rangle$, which obeys the normalization rule:

$$\sum_\lambda \int \frac{d^3\tilde{\mathbf{p}}}{2\tilde{p}_z (2\pi)^3} |\langle\tilde{\mathbf{p}}, \lambda|\Psi\rangle|^2 = 1. \quad (37)$$

The normal mode expansion of the proton field operator is given by:

$$\hat{\psi}(x) = \sum_\lambda \int \frac{d^3\tilde{\mathbf{p}}}{2\tilde{p}_z (2\pi)^3} \left\{ u(\tilde{\mathbf{p}}, \lambda) e^{-i\tilde{\mathbf{p}} \cdot \tilde{x}} b(\tilde{\mathbf{p}}, \lambda) + v(\tilde{\mathbf{p}}, \lambda) e^{+i\tilde{\mathbf{p}} \cdot \tilde{x}} d^\dagger(\tilde{\mathbf{p}}, \lambda) \right\}, \quad (38)$$

where the spinors u and v are normalized such that $\bar{u}(\tilde{\mathbf{p}}, \lambda') u(\tilde{\mathbf{p}}, \lambda) = 2m\delta_{\lambda\lambda'}$ and $\bar{v}(\tilde{\mathbf{p}}, \lambda') v(\tilde{\mathbf{p}}, \lambda) = -2m\delta_{\lambda\lambda'}$ ⁵. Explicit expressions for the spinors can be found in Appendix A. A fully covariant coordinate-representation wave function for a single-proton state can be defined through the field operator as:

$$\Psi_{\text{cov}}(x) = \langle 0 | \hat{\psi}(x) | \Psi \rangle, \quad (39)$$

⁵ We remark for clarity that $\bar{u}(\tilde{\mathbf{p}}, \lambda) = u^\dagger(\tilde{\mathbf{p}}, \lambda) \gamma^0$ and $\bar{v}(\tilde{\mathbf{p}}, \lambda) = v^\dagger(\tilde{\mathbf{p}}, \lambda) \gamma^0$ as usual, and that $\tilde{\gamma}^0$ is not used to define the barred spinors. In the context of defining barred spinors, γ^0 plays the role of swapping left-handed and right-handed components, rather than as the 0th component of a four-vector. Put another way, $\bar{u}(\tilde{\mathbf{p}}', \lambda') u(\tilde{\mathbf{p}}, \lambda)$ is a scalar, and therefore should not change with the transformation from Minkowski to tilted coordinates, meaning the definition of $\bar{u}(\tilde{\mathbf{p}}, \lambda)$ should not change to use $\tilde{\gamma}^0$.

and is related to the momentum-representation wave function through a Fourier transform:

$$\Psi_{\text{cov}}(x) = \sum_{\lambda} \int \frac{d^3 \tilde{\mathbf{p}}}{2\tilde{p}_z(2\pi)^3} u(\tilde{\mathbf{p}}, \lambda) \langle \tilde{\mathbf{p}}, \lambda | \Psi \rangle e^{-i\tilde{\mathbf{p}} \cdot \tilde{\mathbf{x}}} . \quad (40)$$

Through this relation, it can be shown that $\Psi(\tilde{\mathbf{x}}, \tilde{\tau})$ obeys the Dirac equation:

$$(i\tilde{\not{\partial}} - m)\Psi_{\text{cov}}(x) = \sum_{\lambda} \int \frac{d^3 \tilde{\mathbf{p}}}{2\tilde{p}_z(2\pi)^3} (\not{\tilde{p}} - m)u(\tilde{\mathbf{p}}, \lambda) \langle \tilde{\mathbf{p}}, \lambda | \Psi \rangle e^{-i\tilde{\mathbf{p}} \cdot \tilde{\mathbf{x}}} = 0 , \quad (41)$$

where $(\not{\tilde{p}} - m)u(\tilde{\mathbf{p}}, \lambda) = 0$ was used.

A. Helicity-component wave functions

It is helpful to consider helicity components of the proton wave function. These are defined:

$$\Psi_{\lambda}(\tilde{\mathbf{x}}, \tilde{\tau}) = \frac{\bar{u}(i\tilde{\nabla}, \lambda)}{2m} \Psi_{\text{cov}}(x) = \int \frac{d^3 \tilde{\mathbf{p}}}{2\tilde{p}_z(2\pi)^3} \langle \tilde{\mathbf{p}}, \lambda | \Psi \rangle e^{-i\tilde{\mathbf{p}} \cdot \tilde{\mathbf{x}}} , \quad (42)$$

and are given by a Fourier transform of the momentum-representation wave function. From inverting Eq. (42) and placing it into Eq. (37), the following normalization relation can be derived for the helicity components:

$$\sum_{\lambda} \int d^3 \tilde{\mathbf{x}} \Psi_{\lambda}^*(\tilde{\mathbf{x}}, \tilde{\tau}) i \overleftrightarrow{\partial}^0 \Psi_{\lambda}(\tilde{\mathbf{x}}, \tilde{\tau}) = 1 , \quad (43)$$

where $\tilde{\partial}^0 \equiv \tilde{g}^{0\mu} \tilde{\partial}_{\mu}$ and where the two-sided derivative is defined as $f \overleftrightarrow{\partial}_{\mu} g = f(\partial_{\mu} g) - (\partial_{\mu} f)g$. Notably, this appears to be the 0th component of a four-current:

$$\mathcal{P}^{\mu}(\tilde{\mathbf{x}}, \tilde{\tau}) = \sum_{\lambda} \Psi_{\lambda}^*(\tilde{\mathbf{x}}, \tilde{\tau}) i \overleftrightarrow{\partial}^{\mu} \Psi_{\lambda}(\tilde{\mathbf{x}}, \tilde{\tau}) , \quad (44)$$

and it can be confirmed through the help of Eq. (42) that:

$$\tilde{\partial}_{\mu} \mathcal{P}^{\mu}(\tilde{\mathbf{x}}, \tilde{\tau}) = 0 . \quad (45)$$

Thus $\mathcal{P}^{\mu}(\tilde{\mathbf{x}}, \tilde{\tau})$ is a conserved current. As discussed in Sec. II C, $\mathcal{P}^0(\tilde{\mathbf{x}}, \tilde{\tau})$ is thus the density of the conserved “charge” associated with this current. Its normalization to unity confers it an interpretation as a probability density, and thus $\mathcal{P}^{\mu}(\tilde{\mathbf{x}}, \tilde{\tau})$ can be interpreted as the probability four-current.

B. Spin density matrices

Lastly, we define spin-projection densities and currents. In this formulation, we emphasize properties that are invariant under light front boosts and use linear combinations of definite- λ states to define spin densities. In particular, we follow the conventional definitions in the light front literature [37]:

$$|s_z = \pm 1/2\rangle = |\lambda = \pm 1/2\rangle \quad (46a)$$

$$|s_x = \pm 1/2\rangle = \frac{|\lambda = +1/2\rangle \pm |\lambda = -1/2\rangle}{\sqrt{2}} \quad (46b)$$

$$|s_y = \pm 1/2\rangle = \frac{|\lambda = +1/2\rangle \pm i|\lambda = -1/2\rangle}{\sqrt{2}} . \quad (46c)$$

It should be remarked that for systems with non-zero velocity, these are not actually eigenstates of the appropriate components of the Pauli-Lubanski vector. However, for a system at rest, these do become true spin eigenstates. Moreover, these states are invariant under light front boosts, and accordingly can be identified as states with definite spin in their own rest frame.

States with definite spin along the a axis (where $a = x, y, z$) are eigenstates of the Pauli matrix σ_a , and accordingly a spin density can be defined:

$$\mathcal{S}_a(\tilde{\mathbf{x}}, \tilde{\tau}) = \sum_{\lambda\lambda'} \Psi_{\lambda'}^*(\tilde{\mathbf{x}}, \tilde{\tau}) i \overleftrightarrow{\partial}^0 (\sigma_a)_{\lambda'\lambda} \Psi_{\lambda}(\tilde{\mathbf{x}}, \tilde{\tau}). \quad (47)$$

This is essentially a density for the expectation value of σ_a . Just as with the probability density, this is the 0th component of a four-current that is conserved.

Since spin, defined in this manner, is boost-invariant, it is meaningful to consider it an intrinsic property of the system under consideration. It is thus helpful to consider a spin density matrix:

$$\mathcal{P}_{\lambda'\lambda}^{\mu}(\tilde{\mathbf{x}}, \tilde{\tau}) = \Psi_{\lambda'}^*(\tilde{\mathbf{x}}, \tilde{\tau}) i \overleftrightarrow{\partial}^{\mu} \Psi_{\lambda}(\tilde{\mathbf{x}}, \tilde{\tau}), \quad (48)$$

the trace of which gives the probability four-current of Eq. (44). Spin four-currents can similarly be obtained from multiplying by $(\sigma_a)_{\lambda'\lambda}$ and summing over λ, λ' , with the 0th component of this operation reproducing the spin-projection density in Eq. (47).

IV. DERIVATION OF ELECTROMAGNETIC DENSITIES

In this section, we derive the internal electromagnetic densities of the proton when light front time synchronization is used. We closely follow the methodology of Ref. [15]: the physical density is identified as the expectation value of the electromagnetic current operator $\hat{j}^{\mu}(x)$ within a physical state, which is decomposed into a sum of wave-packet-independent internal densities convolved with packet-dependent smearing functions.

A. General formula for the physical electromagnetic current

The physical electromagnetic current is the expectation value of the electromagnetic current operator for a physical state:

$$\langle \tilde{j}^{\mu}(\tilde{x}) \rangle = \langle \Psi | \hat{j}^{\mu}(\tilde{x}) | \Psi \rangle. \quad (49)$$

Using $\hat{j}^{\mu}(\tilde{x}) = e^{i\tilde{P}\cdot\tilde{x}} \hat{j}^{\mu}(0) e^{-i\tilde{P}\cdot\tilde{x}}$ and the one-particle projection operator, we can write:

$$\langle \tilde{j}^{\mu}(\tilde{x}) \rangle = \sum_{\lambda, \lambda'} \int \frac{d^3\tilde{\mathbf{p}}}{2\tilde{p}_z(2\pi)^3} \int \frac{d^3\tilde{\mathbf{p}}'}{2\tilde{p}'_z(2\pi)^3} \Psi^*(\tilde{\mathbf{p}}', \lambda') \langle \tilde{\mathbf{p}}', \lambda' | \hat{j}^{\mu}(0) | \tilde{\mathbf{p}}, \lambda \rangle \Psi(\tilde{\mathbf{p}}, \lambda) e^{i\tilde{\Delta}\cdot\tilde{x}}, \quad (50)$$

where $\tilde{\Delta} = \tilde{\mathbf{p}}' - \tilde{\mathbf{p}}$. Using the inversion of Eq. (42) here gives:

$$\langle \tilde{j}^{\mu}(\tilde{x}) \rangle = \sum_{\lambda, \lambda'} \int d^3\tilde{\mathbf{R}} \int d^3\tilde{\mathbf{R}}' \int \frac{d^3\tilde{\mathbf{P}}}{(2\pi)^3} \int \frac{d^3\tilde{\Delta}}{(2\pi)^3} \Psi_{\lambda'}^*(\tilde{\mathbf{R}}', \tilde{\tau}) \langle \tilde{\mathbf{p}}', \lambda' | \hat{j}^{\mu}(0) | \tilde{\mathbf{p}}, \lambda \rangle \Psi_{\lambda}(\tilde{\mathbf{R}}, \tilde{\tau}) e^{-i\tilde{\Delta}\cdot(\tilde{\mathbf{x}} - \frac{\tilde{\mathbf{R}} + \tilde{\mathbf{R}}'}{2})} e^{i\tilde{P}\cdot(\tilde{\mathbf{R}}' - \tilde{\mathbf{R}})}, \quad (51)$$

where $\tilde{P} = \frac{1}{2}(\tilde{\mathbf{p}} + \tilde{\mathbf{p}}')$. As observed in Refs. [13, 15], the integral over $\tilde{\mathbf{P}}$ can be performed, producing a delta function that sets $\tilde{\mathbf{R}}' = \tilde{\mathbf{R}}$, if the substitutions

$$\tilde{P} \mapsto \frac{i}{2} \overleftrightarrow{\partial} \quad (52)$$

are implicitly made within the matrix element $\langle \tilde{\mathbf{p}}', \lambda' | \hat{j}^{\mu}(0) | \tilde{\mathbf{p}}, \lambda \rangle$. The result is:

$$\langle \tilde{j}^{\mu}(\tilde{x}) \rangle = \sum_{\lambda, \lambda'} \int d^3\tilde{\mathbf{R}} \int \frac{d^3\tilde{\Delta}}{(2\pi)^3} \Psi_{\lambda'}^*(\tilde{\mathbf{R}}, \tilde{\tau}) \langle \tilde{\mathbf{p}}', \lambda' | \hat{j}^{\mu}(0) | \tilde{\mathbf{p}}, \lambda \rangle \Psi_{\lambda}(\tilde{\mathbf{R}}, \tilde{\tau}) e^{-i\tilde{\Delta}\cdot(\tilde{\mathbf{x}} - \tilde{\mathbf{R}})}. \quad (53)$$

The matrix element appearing here can be decomposed into form factors as:

$$\langle \tilde{\mathbf{p}}', \lambda' | \hat{j}^{\mu}(0) | \tilde{\mathbf{p}}, \lambda \rangle = \bar{u}(\tilde{\mathbf{p}}', \lambda') \left\{ \tilde{\gamma}^{\mu} F_1(\Delta^2) + \frac{i\tilde{\sigma}^{\mu\nu}\tilde{\Delta}_{\nu}}{2m} F_2(\Delta^2) \right\} u(\tilde{\mathbf{p}}, \lambda), \quad (54)$$

where we use the normalization convention that $F_2(0) = \kappa$ gives the anomalous magnetic moment. The Lorentz-invariant momentum transfer in tilted coordinates is:

$$\Delta^2 = 2\tilde{\Delta}_z\tilde{\Delta}_0 - \tilde{\Delta}^2 = 2\tilde{\Delta}_z(\tilde{p}'_0 - \tilde{p}_0) - \tilde{\Delta}^2 = 2\tilde{\Delta}_z \left(\frac{m^2 + \left(\tilde{\mathbf{P}} + \frac{1}{2}\tilde{\Delta}\right)^2}{2\tilde{P}_z + \tilde{\Delta}_z} - \frac{m^2 + \left(\tilde{\mathbf{P}} - \frac{1}{2}\tilde{\Delta}\right)^2}{2\tilde{P}_z - \tilde{\Delta}_z} \right) - \tilde{\Delta}^2, \quad (55)$$

which clearly depends on $\tilde{\mathbf{P}}$. This $\tilde{\mathbf{P}}$ dependence causes the argument of the form factors to depend on the wave packet, which provides an obstacle to separating internal structure from wave packet dependence.

As previously observed in Ref. [15], this undesired $\tilde{\mathbf{P}}$ dependence can be eliminated by integrating out \tilde{z} in the physical density. Doing so turns $e^{-i\tilde{\Delta}_z\tilde{z}}$ into a Dirac delta function that sets $\tilde{\Delta}_z = 0$. We are left with a two-dimensional density:

$$\langle \tilde{j}^\mu(\tilde{\mathbf{x}}_\perp, \tilde{\tau}) \rangle_{2D} \equiv \int d\tilde{z} \langle \tilde{j}^\mu(\tilde{x}) \rangle = \sum_{\lambda, \lambda'} \int d^3\tilde{\mathbf{R}} \int \frac{d^2\tilde{\Delta}_\perp}{(2\pi)^2} \Psi_{\lambda'}^*(\tilde{\mathbf{R}}, \tilde{\tau}) \langle \tilde{\mathbf{p}}', \lambda' | \hat{j}^\mu(0) | \tilde{\mathbf{p}}, \lambda \rangle \Psi_\lambda(\tilde{\mathbf{R}}, \tilde{\tau}) e^{-i\tilde{\Delta}_\perp \cdot (\tilde{\mathbf{x}} - \tilde{\mathbf{R}})}, \quad (56)$$

where the substitution of Eq. (52) is still implicitly being applied. With $\tilde{\Delta}_z = 0$, the Lorentz-invariant momentum transfer is just:

$$\Delta^2 = -\tilde{\Delta}_\perp^2. \quad (57)$$

At this point, we can use the explicit spinor elements found in Appendix A to write:

$$\begin{aligned} \langle \tilde{\mathbf{p}}', \lambda' | \hat{j}^\mu(0) | \tilde{\mathbf{p}}, \lambda \rangle = 2\tilde{P}^\mu & \left((\sigma_0)_{\lambda'\lambda} F_1(-\tilde{\Delta}_\perp^2) - \frac{i\epsilon^{\alpha\beta\gamma\delta} \tilde{n}_\alpha \tilde{n}_\beta \tilde{\Delta}_\gamma (\sigma_\delta)_{\lambda'\lambda}}{2m} F_2(-\tilde{\Delta}_\perp^2) \right) \\ & - \frac{i\epsilon^{\mu\nu\rho\sigma} \tilde{n}_\nu \tilde{P}_\rho \tilde{\Delta}_\sigma}{(\tilde{\mathbf{P}} \cdot \tilde{\mathbf{n}})} (\sigma_3)_{\lambda'\lambda} G_M(-\tilde{\Delta}_\perp^2) + \frac{m\tilde{n}^\mu}{(\tilde{\mathbf{P}} \cdot \tilde{\mathbf{n}})} i\epsilon^{\alpha\beta\gamma\delta} \tilde{n}_\alpha \tilde{n}_\beta \tilde{\Delta}_\gamma (\sigma_\delta)_{\lambda'\lambda} G_M(-\tilde{\Delta}_\perp^2), \end{aligned} \quad (58)$$

where $G_M(-\tilde{\Delta}_\perp^2) = F_1(-\tilde{\Delta}_\perp^2) + F_2(-\tilde{\Delta}_\perp^2)$ is the Sachs magnetic form factor, and where $\tilde{n}_\mu = (1; 0, 0, 0)$ and $\tilde{n}^\mu = (1; 0, 0, 0)$ are four-vectors that project out the time component of \tilde{x}^μ and the energy component of \tilde{p}_μ respectively—and in this sense are analogous to the n and \bar{n} vectors used in standard light front coordinates. Noting the substitution rule of Eq. (52), wave packet dependence is indicated by \tilde{P} dependence. The wave packet dependence in the first line of Eq. (58) can be identified as the spin density matrix defined in Eq. (48). For the second line, additional smearing functions must be defined:

$$\mathcal{J}_{\nu, \lambda'\lambda}(\tilde{\mathbf{R}}, \tilde{\tau}) = 2m \Psi_{\lambda'}^*(\tilde{\mathbf{R}}, \tilde{\tau}) \frac{-\tilde{P}_\nu}{(\tilde{\mathbf{P}} \cdot \tilde{\mathbf{n}})} \Psi_\lambda(\tilde{\mathbf{R}}, \tilde{\tau}) \quad (59a)$$

$$\mathcal{K}_{\lambda'\lambda}(\tilde{\mathbf{R}}, \tilde{\tau}) = 2m \Psi_{\lambda'}^*(\tilde{\mathbf{R}}, \tilde{\tau}) \frac{m}{(\tilde{\mathbf{P}} \cdot \tilde{\mathbf{n}})} \Psi_\lambda(\tilde{\mathbf{R}}, \tilde{\tau}), \quad (59b)$$

where factors of $2m$ were introduced so that these functions have the same units as the spin density matrix. If we additionally define the three following internal densities:

$$\rho_{\lambda'\lambda}(\tilde{\mathbf{b}}_\perp) = \int \frac{d^2\tilde{\Delta}_\perp}{(2\pi)^2} \left((\sigma_0)_{\lambda'\lambda} F_1(-\tilde{\Delta}_\perp^2) - \frac{i\epsilon^{\alpha\beta\gamma\delta} \tilde{n}_\alpha \tilde{n}_\beta \tilde{\Delta}_\gamma (\sigma_\delta)_{\lambda'\lambda}}{2m} F_2(-\tilde{\Delta}_\perp^2) \right) e^{-i\tilde{\Delta}_\perp \cdot \tilde{\mathbf{b}}_\perp} \quad (60a)$$

$$j_{\perp, \lambda'\lambda}^{\mu\nu}(\tilde{\mathbf{b}}_\perp) = - \int \frac{d^2\tilde{\Delta}_\perp}{(2\pi)^2} \frac{i\epsilon^{\mu\nu\rho\sigma} \tilde{n}_\rho \tilde{\Delta}_\sigma}{2m} (\sigma_3)_{\lambda'\lambda} G_M(-\tilde{\Delta}_\perp^2) e^{-i\tilde{\Delta}_\perp \cdot \tilde{\mathbf{b}}_\perp} \quad (60b)$$

$$j_{\parallel, \lambda'\lambda}^\mu(\tilde{\mathbf{b}}_\perp) = \int \frac{d^2\tilde{\Delta}_\perp}{(2\pi)^2} \frac{i\epsilon^{\alpha\beta\gamma\delta} \tilde{n}_\alpha \tilde{n}_\beta \tilde{\Delta}_\gamma (\sigma_\delta)_{\lambda'\lambda}}{2m} \tilde{n}^\mu G_M(-\tilde{\Delta}_\perp^2) e^{-i\tilde{\Delta}_\perp \cdot \tilde{\mathbf{b}}_\perp}, \quad (60c)$$

then the physical density can be written as:

$$\begin{aligned} \langle \tilde{j}^\mu(\tilde{\mathbf{x}}_\perp, \tilde{\tau}) \rangle_{2D} = \sum_{\lambda, \lambda'} \int d^3\tilde{\mathbf{R}} & \left\{ \mathcal{P}_{\lambda'\lambda}^\mu(\tilde{\mathbf{R}}, \tilde{\tau}) \rho_{\lambda'\lambda}(\tilde{\mathbf{x}}_\perp - \tilde{\mathbf{R}}_\perp) \right. \\ & \left. + \mathcal{J}_{\nu, \lambda'\lambda}(\tilde{\mathbf{R}}, \tilde{\tau}) j_{\perp, \lambda'\lambda}^{\mu\nu}(\tilde{\mathbf{x}}_\perp - \tilde{\mathbf{R}}_\perp) + \mathcal{K}_{\lambda'\lambda}(\tilde{\mathbf{R}}, \tilde{\tau}) j_{\parallel, \lambda'\lambda}^\mu(\tilde{\mathbf{x}}_\perp - \tilde{\mathbf{R}}_\perp) \right\}. \end{aligned} \quad (61)$$

With the general expression now in hand, we must now investigate the meaning of the internal densities in Eq. (60).

B. Interpretation of internal densities

Let us now consider the interpretation of the internal densities in Eq. (60), with a special focus on the spatial structure of the proton in its rest frame. Although there is no rest state of the proton in Hilbert space—since wave functions must necessarily be square integrable—we will show that the internal densities are boost-invariant quantities, and that artifacts of the proton's motion have all been absorbed into the smearing functions in Eq. (61). Moreover, these interpretations can be further validated by utilizing the rest condition $\mathbf{P} = (0, 0, m)$ found in Eq. (15).

We shall consider states with definite light front spin $\frac{1}{2}\hat{s}$ —as described in Sec. III B—since these correspond to a proton with definite spin in its own rest frame. For these states, one can substitute:

$$(\sigma_0)_{\lambda'\lambda} \mapsto 1 \quad (62a)$$

$$(\sigma_i)_{\lambda'\lambda} \mapsto \hat{s}_i \quad (62b)$$

in the formulas of Eqs. (48), (59) and (60) to obtain spin-state densities, which will now be functions of \hat{s} instead of λ and λ' .

1. Internal charge density

We consider the charge density first. As discussed in Sec. II C, the charge density can be identified by contracting the electromagnetic current with \tilde{n}_μ , giving the 0th component. Since $j_\perp^{0\nu}(\tilde{\mathbf{b}}_\perp, \hat{s}) = 0$ and $j_\parallel^0(\tilde{\mathbf{b}}_\perp, \hat{s}) = 0$ are both zero—a result that is frame-independent, since boosts do not mix spatial components into light front time (see Sec. II B)—the internal charge density is given entirely by:

$$\rho(\tilde{\mathbf{b}}_\perp, \hat{s}) = \int \frac{d^2\tilde{\Delta}_\perp}{(2\pi)^2} \left(F_1(-\tilde{\Delta}_\perp^2) + \frac{(\hat{s} \times i\tilde{\Delta}_\perp) \cdot \hat{z}}{2m} F_2(-\tilde{\Delta}_\perp^2) \right) e^{-i\tilde{\Delta}_\perp \cdot \tilde{\mathbf{b}}_\perp}, \quad (63)$$

where Eq. (A10) was used to rewrite the terms multiplying $F_2(-\tilde{\Delta}_\perp^2)$. Notably, this reproduces the results of Refs. [16, 38, 39] for longitudinally-polarized nucleons, and (up to a sign discrepancy) the results of Carlson and Vanderhaegen [37] for transversely-polarized nucleons⁶. This internal charge density is smeared over space by the probability current, as expected and as previously observed for spin zero targets [15]. This probability current transforms as a Lorentz four-vector, and effectively absorbs all of the boost dependence of the charge density contribution to the physical electromagnetic four-current. Since the spin degrees of freedom are characterized by light front helicity, and since $\tilde{\mathbf{b}}_\perp = \tilde{\mathbf{x}}_\perp - \tilde{\mathbf{R}}_\perp$ is given by a difference between transverse spatial coordinates, the internal density $\rho(\tilde{\mathbf{b}}_\perp, \hat{s})$ is fully invariant under both transverse and longitudinal boosts, and therefore characterizes the internal charge density of the proton in every reference frame—including its rest frame.

2. Transverse current density

We next consider the density $j_\perp^{\mu\nu}(\tilde{\mathbf{b}}_\perp, \hat{s})$. Like the internal charge density, it is boost-invariant, with boost dependence having been absorbed into the smearing function $\mathcal{J}_\nu(\tilde{\mathbf{R}}, \tilde{\tau}, \hat{s})$. The presence of \tilde{n}_ρ in its definition ensures that the $\mu = 0$ and $\nu = 0$ components are all zero. The index μ signifies which component of the physical four-current this density contributes to, and ν signifies which component of the total four-momentum this density is to be contracted with. With the help of Eq. (A10), we can write out the non-zero components as:

$$j_\perp^{23}(\tilde{\mathbf{b}}_\perp, \hat{s}) = -j_\perp^{32}(\tilde{\mathbf{b}}_\perp, \hat{s}) = +\hat{s} \cdot \hat{z} \int \frac{d^2\tilde{\Delta}_\perp}{(2\pi)^2} \frac{i\tilde{\Delta}_x}{2m} G_M(-\tilde{\Delta}_\perp^2) e^{-i\tilde{\Delta}_\perp \cdot \tilde{\mathbf{b}}_\perp} \quad (64a)$$

$$j_\perp^{13}(\tilde{\mathbf{b}}_\perp, \hat{s}) = -j_\perp^{31}(\tilde{\mathbf{b}}_\perp, \hat{s}) = -\hat{s} \cdot \hat{z} \int \frac{d^2\tilde{\Delta}_\perp}{(2\pi)^2} \frac{i\tilde{\Delta}_y}{2m} G_M(-\tilde{\Delta}_\perp^2) e^{-i\tilde{\Delta}_\perp \cdot \tilde{\mathbf{b}}_\perp}. \quad (64b)$$

These entail, first of all, of a transverse current density:

$$\mathbf{j}_\perp(\tilde{\mathbf{b}}_\perp, \hat{s}) = (\hat{s} \cdot \hat{z}) \int \frac{d^2\tilde{\Delta}_\perp}{(2\pi)^2} \frac{(\hat{z} \times i\tilde{\Delta}_\perp)}{2m} G_M(-\tilde{\Delta}_\perp^2) e^{-i\tilde{\Delta}_\perp \cdot \tilde{\mathbf{b}}_\perp}, \quad (65)$$

⁶ The sign discrepancy is due to a mistake in Eq. (1) of Ref. [37], where the complex exponential should be $e^{-i\mathbf{q}_\perp \cdot \tilde{\mathbf{b}}_\perp}$ instead of $e^{i\mathbf{q}_\perp \cdot \tilde{\mathbf{b}}_\perp}$. The sign mistake originated in Ref. [38], where only helicity states were considered so that this sign flip had no effect on its results.

which, considering Eq. (59), is smeared over the transverse plane by the square of the wave function. This smearing function is boost-invariant, meaning the contribution of $j_\perp(\tilde{\mathbf{b}}_\perp, \hat{\mathbf{s}})$ to the physical transverse current density is frame-independent. This density can therefore be identified as the intrinsic transverse current density of the proton, applicable to all frames including the rest frame of the proton.

In addition, the $\mu = 3$ components of $j_\perp^{\mu\nu}(\tilde{\mathbf{b}}_\perp, \hat{\mathbf{s}})$ entail a longitudinal current density:

$$j_{\text{ind},i}^3(\tilde{\mathbf{b}}_\perp, \hat{\mathbf{s}}) = (\hat{\mathbf{s}} \cdot \hat{\mathbf{z}}) \int \frac{d^2 \tilde{\Delta}_\perp}{(2\pi)^2} \frac{(i \tilde{\Delta}_\perp \times \hat{\mathbf{z}})_i}{2m} G_M(-\tilde{\Delta}_\perp^2) e^{-i \tilde{\Delta}_\perp \cdot \tilde{\mathbf{b}}_\perp}, \quad (66)$$

which—considering Eq. (59)—must be contracted with the expectation value of the transverse velocity $(\tilde{\mathbf{P}}_\perp/\tilde{P}_z)_i$ to give a contribution to the physical longitudinal current. The smearing function associated with this contribution is not boost invariant, and in fact vanishes in a frame where the expectation value of the transverse velocity is zero. In fact, an intrinsic transverse current can induce a longitudinal current under transverse boosts, since transverse boosts mix transverse spatial coordinates into the z coordinate—see Eq. (19). Since $j_{\text{ind},i}^3(\tilde{\mathbf{b}}_\perp, \hat{\mathbf{s}})$ vanishes in a frame where the expected value of the transverse velocity is zero, we call it a boost-induced longitudinal current, in contrast to an intrinsic longitudinal current. We shall address the intrinsic longitudinal current density next.

3. Longitudinal current density

The last intrinsic density defined in Eq. (60) is j_\parallel^μ . Considering $\tilde{n}^\mu = (0; 0, 0, -1)$, the only component is $\mu = 3$, which for definite-spin states can be written (with the help of Eq. (A10)):

$$j_\parallel^3(\tilde{\mathbf{b}}_\perp, \hat{\mathbf{s}}) = \int \frac{d^2 \tilde{\Delta}_\perp}{(2\pi)^2} \frac{(\hat{\mathbf{s}} \times i \tilde{\Delta}_\perp) \cdot \hat{\mathbf{z}}}{2m} G_M(-\tilde{\Delta}_\perp^2) e^{-i \tilde{\Delta}_\perp \cdot \tilde{\mathbf{b}}_\perp}. \quad (67)$$

This is smeared over the transverse plane by the function $\mathcal{H}(\tilde{\mathbf{R}}, \tilde{\tau}, \hat{\mathbf{s}})$ defined in Eq. (59), which is invariant under the Galilean subgroup (including transverse boosts) but not under longitudinal boosts. Under an *active* boost of rapidity η , the smearing function scales as $e^{-\eta}$, meaning the longitudinal current is redshifted (slowed down) for $\eta > 0$ and blueshifted (sped up) for $\eta < 0$. We remind the reader that $\eta > 0$ increases \tilde{P}_z and has the system move away from the observer, while $\eta < 0$ decreases \tilde{P}_z and has the system move towards the observer, assuming it is located upstream from (at a larger \tilde{z} coordinate than) the observer.

Although the intrinsic transverse current and intrinsic longitudinal current are separated in our formulation—the separation being necessary by virtue of the different transformation properties of their smearing functions under boosts—we may choose to formally combine Eqs. (65) and (67) into a single expression for the intrinsic electric current:

$$\tilde{\mathbf{j}}(\tilde{\mathbf{b}}_\perp, \hat{\mathbf{s}}) = \int \frac{d^2 \tilde{\Delta}_\perp}{(2\pi)^2} \frac{\hat{\mathbf{s}} \times i \tilde{\Delta}_\perp}{2m} G_M(-\tilde{\Delta}_\perp^2) e^{-i \tilde{\Delta}_\perp \cdot \tilde{\mathbf{b}}_\perp}. \quad (68)$$

V. EMPIRICAL REST FRAME CHARGE AND CURRENT DENSITIES

Using the results from Sec. IV, we proceed to present numerical results for the internal rest frame densities of the proton and the neutron. For $F_1(\Delta^2)$ and $F_2(\Delta^2)$, we use the parametrizations fit to empirical data by Kelly [40], combined with improved measurements of the neutron electric form factor by Riordan *et al.* [41].

We first present results for the rest frame charge densities in Fig. 3, which can all be calculated using Eq. (63). The neutron charge density for helicity states reproduces the finding of Miller [38], in which the neutron has a negatively-charged core surrounded by a diffuse cloud of positive charge. The charge densities for transversely-polarized states reproduce the previous results of Carlson and Vanderhaegen [37] up to the previously noted sign discrepancy in the $\sin \phi$ modulations.

It is worth emphasizing that we have reproduced and affirmed previously-known results for the transverse charge density in the standard light front formalism. These previous results were found to be entirely frame-independent, with the spin degree of freedom specifically quantifying the nucleon's spin in its own rest frame. The limit of infinite momentum was never considered or taken. It is mistaken to attribute features of these densities to kinematic effects from boosting to infinite momentum. The cause of angular modulations in the densities of transversely-polarized states must lie elsewhere, and in fact originates from the time synchronization convention. We shall comment on this further in Sec. VB.

For now, we further remark that the angular modulations in the charge densities of transversely-polarized states produce an effective electric dipole moment, which can be calculated from Eq. (63) as follows:

$$\mathbf{p}_{\text{eff}} \equiv \int d^2 \tilde{\mathbf{b}}_\perp \tilde{\mathbf{b}}_\perp \rho_{\text{rest}}(\tilde{\mathbf{b}}_\perp, \hat{\mathbf{s}}) = \frac{\hat{\mathbf{z}} \times \hat{\mathbf{s}}}{2m} F_2(0) = (\hat{\mathbf{z}} \times \hat{\mathbf{s}}) \frac{\kappa}{2m}, \quad (69)$$

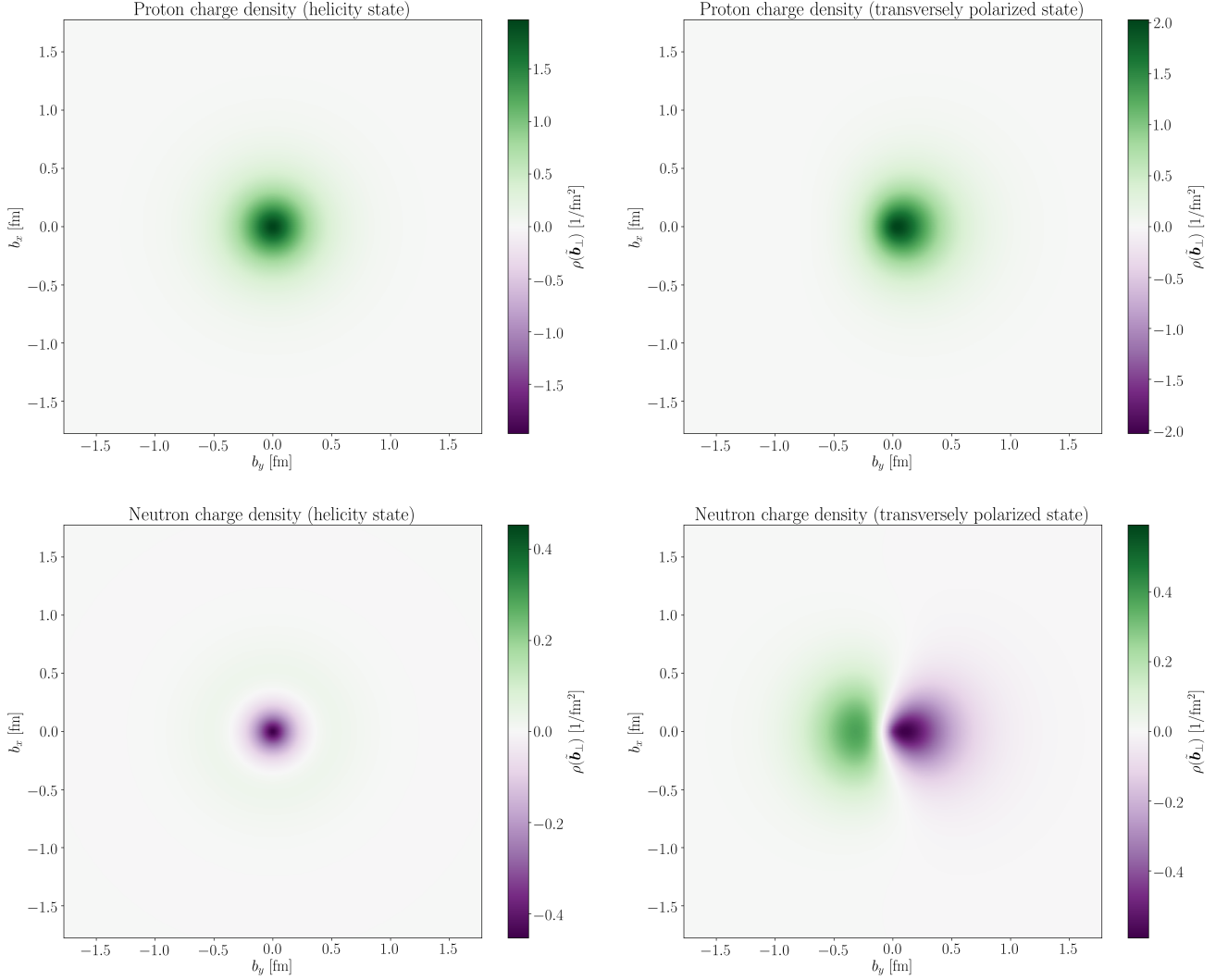


FIG. 3. Rest frame charge densities of the proton (top row) and neutron (bottom row). The left column depicts positive-helicity states (spin-up along the z axis), while the right column depicts transversely-polarized states with spin up along the x axis.

where κ is the anomalous magnetic moment of the nucleon. Since it is an effect of using light front synchronization, we call this a synchronization-induced electric dipole moment. From the empirical values of the masses and anomalous magnetic moments, the induced dipole moments of the proton and neutron are:

$$p_p = 0.19 \text{ fm} \quad (70a)$$

$$p_n = -0.20 \text{ fm} . \quad (70b)$$

We next present in Fig. 4 numerical results for the internal electric current distributions of the proton and neutron. It should be noted that we use a right-handed coordinate system in these plots in which the x axis is oriented vertically and the y axis is oriented horizontally, so that the z axis points into the page. This choice is made so that the distributions reflect what an observer located downstream from the target (i.e., at a lesser z coordinate) actually sees. The clockwise revolution of the electric current for a proton with spin up along the z axis (top left panel) thus entails a positive magnetic moment, while the counterclockwise revolution of a neutron in the same state (bottom left panel) entails a negative magnetic moment. The helicity-state results in the left column reproduce the findings of Chen and Lorcé [14].

For a transversely polarized nucleon, the only non-zero component of its internal current density—as defined in Eq. (68)—is $\tilde{j}^3(\mathbf{b}_\perp)$. This is depicted in the right column of Fig. 4. That the z axis points into the page is worth emphasizing when interpreting these plots. For a proton that is spin-up along the x axis, the current is moving towards the observer at $b_y < 0$ and away from the observer at $b_y > 0$. Since the observer looks in the $+z$ direction, a current towards the observer is negative. Using the

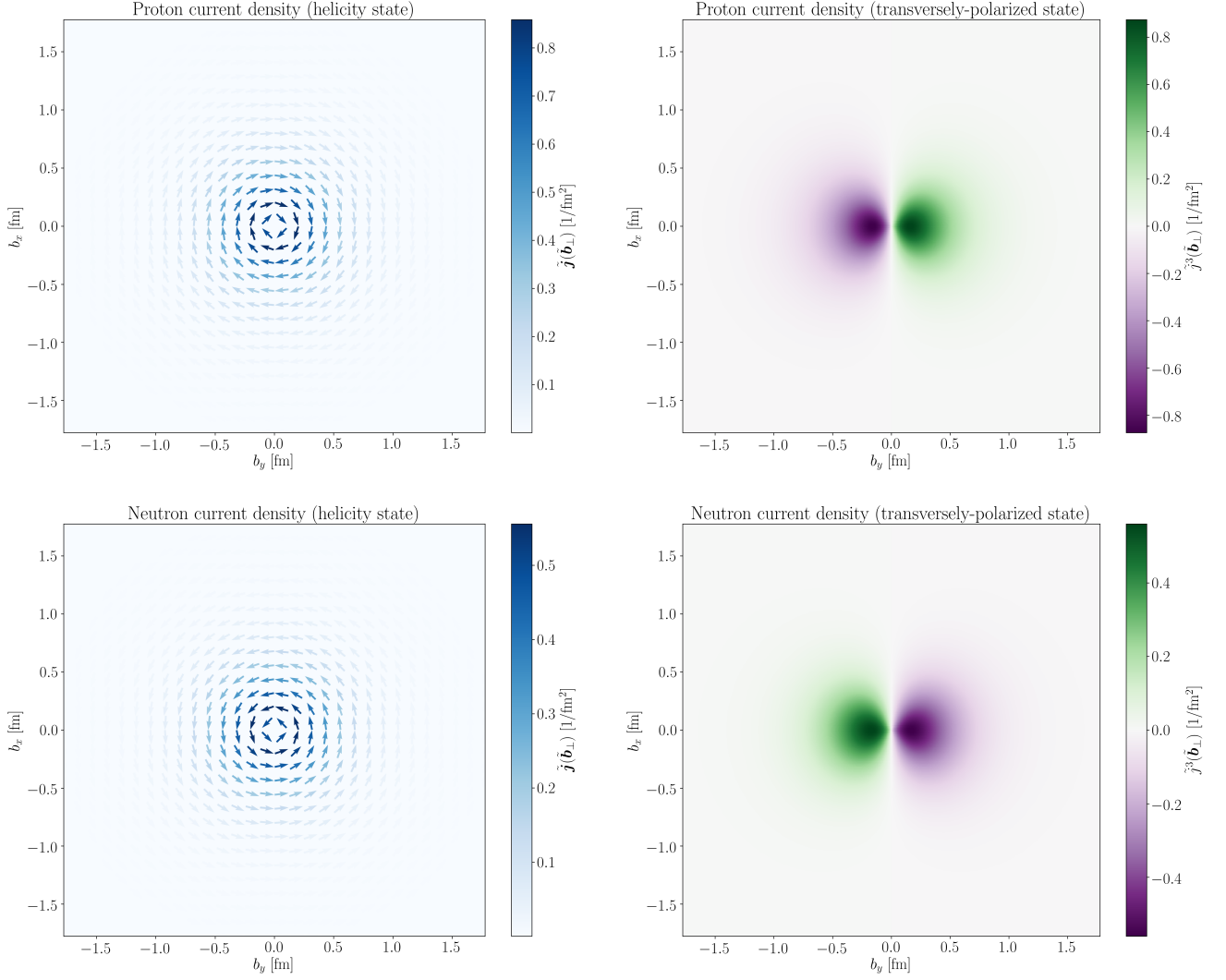


FIG. 4. Rest frame electric current distributions in the proton (top row) and neutron (bottom row). The left column depicts positive-helicity states (spin-up along the z axis), while the right column depicts transversely-polarized states with spin up along the x axis. These figures use a right-handed coordinate system with a vertical x axis and horizontal y axis, so the z axis points into the page.

right-hand rule, the transversely-polarized proton (top-right panel) has an electric current that co-revolves with its spin, while the transversely-polarized neutron (bottom-right panel) has an electric current that counter-rotates against its spin. These are consistent with the picture suggested by the helicity-state nucleons.

It is worth remarking that the $\tilde{j}^3(\tilde{\mathbf{b}}_\perp)$ results for transversely-polarized states are new, and could be obtained and meaningfully interpreted by virtue of using tilted coordinates instead of standard light front coordinates.

A. Quark densities and currents

Information about the densities and currents of up quarks and down quarks in the proton can be found by invoking charge symmetry. The u and d densities in the proton are assumed equal to the d and u densities in the neutron. Thus, for any density $\rho(\tilde{\mathbf{b}}_\perp)$,

$$\rho_p(\tilde{\mathbf{b}}_\perp) = e_u \rho_u(\tilde{\mathbf{b}}_\perp) + e_d \rho_d(\tilde{\mathbf{b}}_\perp) = \frac{2}{3} \rho_u(\tilde{\mathbf{b}}_\perp) - \frac{1}{3} \rho_d(\tilde{\mathbf{b}}_\perp) \quad (71a)$$

$$\rho_n(\tilde{\mathbf{b}}_\perp) = e_u \rho_d(\tilde{\mathbf{b}}_\perp) + e_d \rho_u(\tilde{\mathbf{b}}_\perp) = \frac{2}{3} \rho_d(\tilde{\mathbf{b}}_\perp) - \frac{1}{3} \rho_u(\tilde{\mathbf{b}}_\perp), \quad (71b)$$

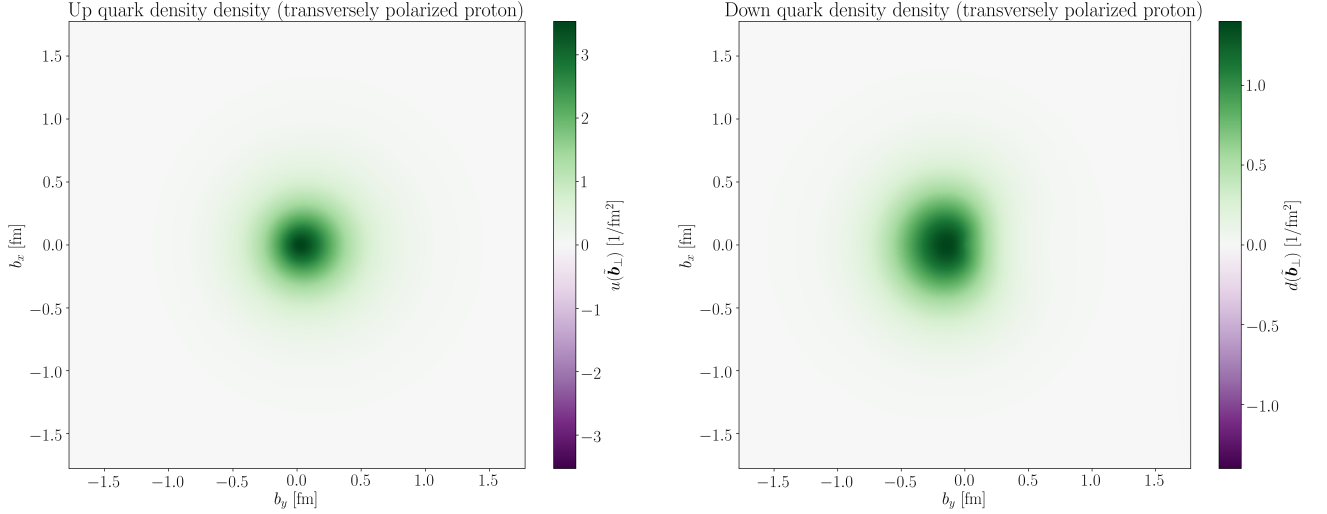


FIG. 5. Rest frame quark densities in a transversely-polarized proton. Rest frame electric densities of the proton (top row) and neutron (bottom row). The proton has spin-up along the x axis. The left panel is the up quark density and the right panel is the down quark density.

n_u	n_d	$\langle(\tilde{\mathbf{b}}_\perp^2)_u\rangle$	$\langle(\tilde{\mathbf{b}}_\perp^2)_d\rangle$	κ_u	κ_d
2	1	$(0.65 \text{ fm})^2$	$(0.68 \text{ fm})^2$	1.68	-2.03

TABLE I. Static quantities associated with up and down quarks in the proton.

which invert to:

$$\rho_u(\tilde{\mathbf{b}}_\perp) = 2\rho_p(\tilde{\mathbf{b}}_\perp) + \rho_n(\tilde{\mathbf{b}}_\perp) \quad (72a)$$

$$\rho_d(\tilde{\mathbf{b}}_\perp) = 2\rho_n(\tilde{\mathbf{b}}_\perp) + \rho_p(\tilde{\mathbf{b}}_\perp). \quad (72b)$$

The up and down quark densities in a helicity-state proton were found previously by Miller [38]. We are now equipped to additionally provide quark densities in transversely-polarized protons, as well as the quark current densities.

Up and down quark densities in a transversely-polarized proton at rest are presented in Fig. 5. These densities are not weighted by charge, so they are positive-definite number densities, normalized to $n_u = 2$ and $n_d = 1$ respectively. Both densities are off-center, but the down quark density is much further displaced from the center. These displacements are in opposite directions, and since the up and down quarks have opposite charge, they make constructive contributions to the synchronization-induced electric dipole moment.

Up and down quark current distributions in a proton are presented in Fig. 6. These are not weighted by charge, so the direction of the current is the genuine direction of motion of the respective quark flavor. For both the longitudinally and transversely-polarized state, the up quark current is in the direction of proton spin, while the down quark current is in the opposite direction. This seems to conflict with model calculations [42, 43] and lattice QCD results [44] finding that up quarks carry negative orbital angular momentum (OAM) and down quarks carry positive OAM, at least at renormalization scales of a few GeV^2 or higher. However, the OAM contains sea quark contributions—hence its renormalization scale dependence—while the quark currents describe only valence quark contributions. This conflict is resolved if the majority of OAM is carried by sea quarks.

We remark, in comparing Fig. 5 to Fig. 6, that each quark density appears to be enhanced where the quarks are moving away from the observer (on the right side of the transversely-polarized plots of up quark distributions, or the left side for down quark distributions), and conversely suppressed where the quarks are moving towards the observer. This is a natural consequence of using light front time synchronization, and will be explored further in Sec. VB.

In Table I, we present individual quark flavors' contributions to the static quantities associated with the proton's charge and current distributions. The quark number, quark radius, and quark contribution to the anomalous magnetic moment (without

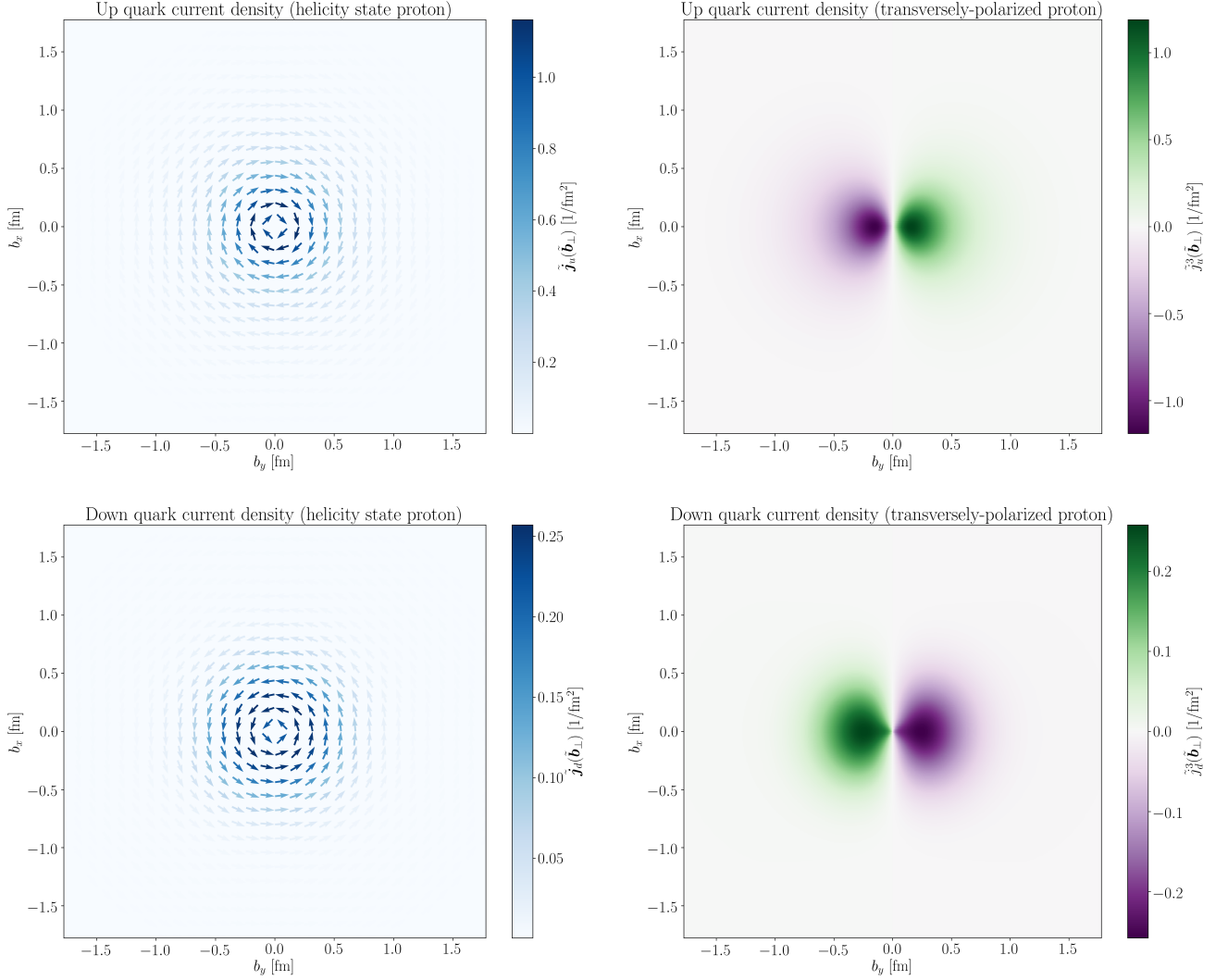


FIG. 6. Rest frame quark current distributions in the proton. Up distributions (top row) and down distributions (bottom row) are shown. The left column depicts positive-helicity states (spin-up along the z axis), while the right column depicts transversely-polarized states with spin up along the x axis. These figures use a right-handed coordinate system with a vertical x axis and horizontal y axis, so the z axis points into the page.

charge weight) are respectively:

$$n_q = F_{1q}(0) \quad (73a)$$

$$\langle (\tilde{\mathbf{b}}_\perp^2)_q \rangle = \frac{4}{F_{1q}(0)} \left. \frac{dF_{1q}(t)}{dt} \right|_{t=0} \quad (73b)$$

$$\kappa_q = F_{2q}(0). \quad (73c)$$

B. Discussion and further interpretation

We now further discuss the interpretation of the internal densities we have obtained, with a special focus on the angular modulations in the charge densities of transversely-polarized nucleons (right column of Fig. 3). Since these densities are frame-invariant and therefore describe a proton even at rest, they cannot be attributed to kinematic effects from boosting to infinite momentum.

Modulations such as these can appear for spinning targets at rest by virtue of using light front synchronization. What a downstream observer sees at any fixed light front time $\tilde{\tau}$ is everything that a single light front encounters while traveling in the

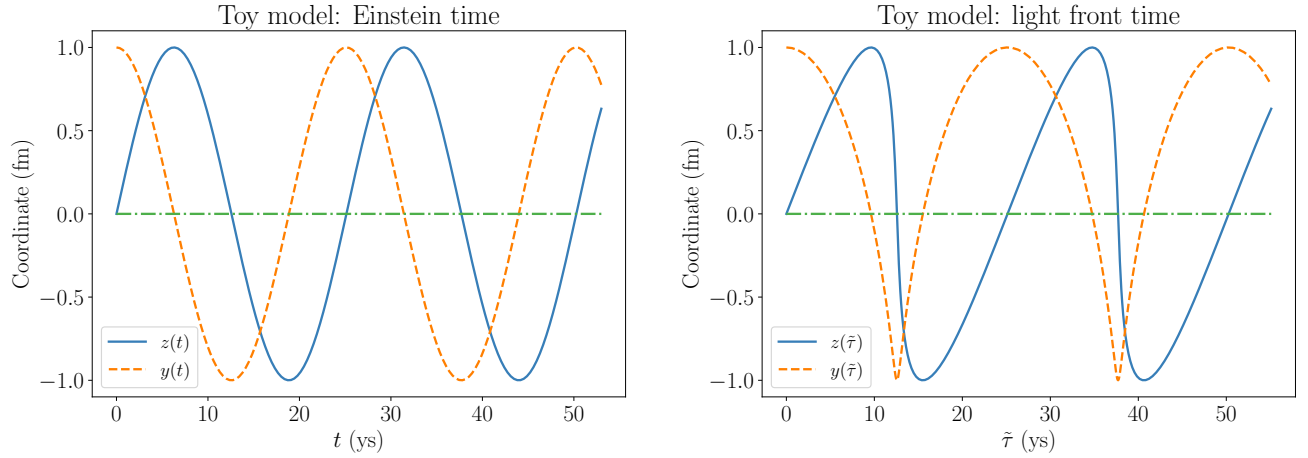


FIG. 7. y and z coordinates of the toy revolver model as functions of Einstein time (left panel) and light front time (right panel), for $R = 1$ fm and $\omega = 250$ ZHh.

$-z$ direction. For an extended rotating body, the light front takes a non-zero amount of Einstein time t to cross the extent of the body, and particles within it will advance in their motion while the light front is crossing it. Particles are more likely to encounter the light front while they're moving against it (in the $+z$ direction), so the particle density will be skewed in the $\hat{z} \times \hat{s}$ direction. This can explain the direction of the modulations in of Figs. 3 and 5, as well as the sign of the synchronization-induced electric dipole moment in Eq. (69).

This same phenomenon can also be rephrased in the language of light front time $\tilde{\tau}$. Suppose that a particle revolves around a transversely-polarized body, taking the same amount of time from its own perspective to reach the lowest- z point of its orbit and the highest- z point of its orbit. Since its time is dilated when moving in the $+z$ direction and quickened when moving in the $-z$ direction from the perspective of a stationary observer (see discussion in Sec. II B), it will spend less time moving towards the observer and more time moving away from the observer from the observer's perspective. This makes it more likely that the observer will see the particle when it's in the $\hat{z} \times \hat{s}$ direction, again skewing the particle density in that direction.

This can be explicitly illustrated in a simple classical toy model. Suppose we have a charged body revolving around a central point with angular velocity ω . The revolution is around the x -axis, and the trajectory in terms of Einstein time t is:

$$\mathbf{r}(t) = R(\hat{y} \cos(\omega t) + \hat{z} \sin(\omega t)). \quad (74)$$

At any Einstein time, the z coordinate is:

$$z(t) = \hat{z} \cdot \mathbf{r}(t) = R \sin(\omega t). \quad (75)$$

The light front time $\tilde{\tau}$ and Einstein time are related by:

$$\tilde{\tau} = t + \frac{z(t)}{c} \equiv t + \frac{\tilde{z}(\tilde{\tau})}{c}, \quad (76)$$

so that the z coordinate as a function of the light front time $\tilde{\tau}$ is given by the implicit formula:

$$\tilde{z}(\tilde{\tau}) = R \sin(\omega[\tilde{\tau} - \tilde{z}(\tilde{\tau})]). \quad (77)$$

The function $\tilde{z}(\tilde{\tau})$ can be solved for numerically. Additionally, from this one can find the y coordinate as a function of light front time from this:

$$\tilde{y}(\tilde{\tau}) = y(t) = R \cos(\omega[\tilde{\tau} - \tilde{z}(\tilde{\tau})]). \quad (78)$$

Numerical results for the revolver coordinates as a function of light front time $\tilde{\tau}$ are presented in the right panel of Fig. 7, with the Einstein time trajectory given in the left panel for contrast. In terms of Einstein time t , the coordinates are simple sinusoids, as expected. In terms of light front time, however, the trajectory appears highly distorted. The revolver spends most of its time moving away from the observer with a low velocity, and then quickly swings back towards the observer at a high velocity in

a short span of light front time. Because of this, the revolver is at a positive y coordinate for longer than it is at a negative y coordinate, and the light-front-time-averaged y coordinate is non-zero. In fact, this average can be calculated analytically:

$$\langle \tilde{y}(\tilde{\tau}) \rangle_{\text{LF}} \equiv \lim_{T \rightarrow \infty} \frac{1}{2\tilde{\tau}(T)} \int_{-\tilde{\tau}(T)}^{+\tilde{\tau}(T)} d\tilde{\tau}' \tilde{y}(\tilde{\tau}') = \lim_{T \rightarrow \infty} \frac{1}{2T + 2\frac{R}{c} \sin(\omega T)} \int_{-T}^{+T} dt \frac{d\tilde{\tau}(t)}{dt} y(t) = \frac{R^2 \omega}{2c}. \quad (79)$$

We can use this model to give an extremely rough estimate of how quickly the valence up and down quarks revolve around the proton. These estimates will be rough because quarks do not orbit the proton in well-defined circular trajectories, but they should give an idea of the order of magnitude of the angular frequency of quark revolutions. If $n_q \langle \tilde{y}(\tilde{\tau}) \rangle_{\text{LF}}$ is interpreted as the synchronization-induced dipole moment of the quark distribution, then using this with Eq. (69) gives:

$$\omega_q = \frac{c \kappa_q}{m_p n_q R_q^2}. \quad (80)$$

For the sake of these estimates, the mean-squared radii given in Table I can be used in place of R_q^2 . Doing this gives the following rough estimates:

$$\omega_u \approx 0.417 \text{ c/fm} = 125 \text{ ZHz} \quad (81a)$$

$$\omega_d \approx -0.922 \text{ c/fm} = -276 \text{ ZHz}, \quad (81b)$$

where the minus sign for the down quark's angular frequency indicates revolution in the opposite direction. These exact numbers depended on a simplistic toy model and should be taken only to give a ballpark estimate of the angular velocity of up and down quarks' orbits around the proton.

VI. CONCLUSIONS AND OUTLOOK

In this work, we used tilted light front coordinates—light front time x^+ and ordinary spatial coordinates (x, y, z) —to demonstrate that the formalism for light front densities follows from use of a peculiar time synchronization convention, rather than from boosting to infinite momentum. Internal densities of electric charge and currents, as well as up and down quark densities and currents, were obtained for a proton. These densities are boost-invariant, and thus describe a proton in any state of motion, including at rest. The densities and transverse currents we obtained reproduced prior results, while the longitudinal current densities were newly-obtained by virtue of using tilted coordinates.

This formalism is equally applicable to the energy-momentum tensor (EMT), allowing all sixteen of its components to be given a clear physical meaning. This will become the subject of a sequel paper. Care will need to be taken about upper and lower indices; since the energy and momentum are identified as covariant components of \tilde{p}_μ (as discussed in Sec. II A), and since the EMT is conserved with respect to its first index, the tilted energy density for instance will be given by:

$$\tilde{T}^0_0 = \tilde{T}^{00} - \tilde{T}^{03} = T^{00} + T^{30}, \quad (82)$$

which involves off-diagonal components of the EMT. For spin-half targets in particular, the energy density may differ depending on whether the EMT contains the antisymmetric piece discussed in Refs. [2, 45]. Tilted light front coordinates will be helpful not only in defining relativistically exact densities for all components of the EMT—including an energy density that integrates to the usual instant form energy E —but may also provide additional insight into the question of whether the physical EMT contains an antisymmetric piece.

ACKNOWLEDGMENTS

The authors would like to thank Ian Cloët, Wim Cosyn, and Yang Li for helpful discussions that contributed to this work. This work was supported by the U.S. Department of Energy Office of Science, Office of Nuclear Physics under Award Number DE-FG02-97ER-41014.

Appendix A: Explicit light front helicity spinors

To evaluate internal proton densities, we will need to evaluate explicit spinor matrix elements. To this end, it is helpful to have explicit expressions for light front helicity spinors. Explicit expressions for these spinors were found already by Kogut and Soper [46]—the Kogut-Soper spinors are in fact eigenstates of the light front helicity operator $\hat{\lambda}$ defined in Eq. (25).

In terms of tilted momentum components, the Kogut-Soper spinors can be written:

$$u\left(\tilde{\mathbf{p}}, +\frac{1}{2}\right) = \frac{1}{\sqrt{\tilde{p}_z}} \begin{bmatrix} \tilde{p}_z \\ \tilde{p}_x + i\tilde{p}_y \\ m \\ 0 \end{bmatrix}, \quad u\left(\tilde{\mathbf{p}}, -\frac{1}{2}\right) = \frac{1}{\sqrt{\tilde{p}_z}} \begin{bmatrix} 0 \\ m \\ -\tilde{p}_x + i\tilde{p}_y \\ \tilde{p}_z \end{bmatrix}. \quad (\text{A1})$$

In this basis, the tilted gamma matrices can be written in block matrix form as:

$$\tilde{\gamma}^0 = \begin{bmatrix} 0 & \mathbb{1} - \sigma_3 \\ \mathbb{1} + \sigma_3 & 0 \end{bmatrix}, \quad \tilde{\gamma}^i = \begin{bmatrix} 0 & -\sigma_i \\ \sigma_i & 0 \end{bmatrix}, \quad (\text{A2})$$

where $\mathbb{1}$ is a 2×2 identity matrix and σ_i are the usual 2×2 Pauli matrices.

The barred spinors are defined as usual by:

$$\bar{u}(\tilde{\mathbf{p}}, \lambda) = u^\dagger(\tilde{\mathbf{p}}, \lambda) \gamma^0 \quad (\text{A3a})$$

$$\bar{v}(\tilde{\mathbf{p}}, \lambda) = v^\dagger(\tilde{\mathbf{p}}, \lambda) \gamma^0 \quad (\text{A3b})$$

where the untilted γ^0 matrix is given by:

$$\gamma^0 = \begin{bmatrix} 0 & \mathbb{1} \\ \mathbb{1} & 0 \end{bmatrix}. \quad (\text{A4})$$

The reason that γ^0 rather than $\tilde{\gamma}^0$ is used is that γ^0 plays the role here of swapping left-handed and right-handed components of the spinor, rather than of isolating a component of a four-vector. Indeed, since $\bar{u}(\tilde{\mathbf{p}}', \lambda') u(\tilde{\mathbf{p}}, \lambda) = u^\dagger(\tilde{\mathbf{p}}', \lambda') \gamma^0 u(\tilde{\mathbf{p}}, \lambda)$ is a scalar, it should be invariant under the transformation from Minkowski to tilted coordinates.

It is helpful to have explicit matrix elements of spinors, in particular when momentum in the z direction remains unchanged. Let $\tilde{\mathbf{p}} = \tilde{\mathbf{P}} - \frac{1}{2}\tilde{\mathbf{\Delta}}$ and $\tilde{\mathbf{p}}' = \tilde{\mathbf{P}} + \frac{1}{2}\tilde{\mathbf{\Delta}}$, and $\tilde{\Delta}_z = 0$. For equal-helicity spinors, we find the following matrix elements:

$$\bar{u}(\tilde{\mathbf{p}}', \lambda) u(\tilde{\mathbf{p}}, \lambda) = 2m \quad (\text{A5a})$$

$$\bar{u}(\tilde{\mathbf{p}}', \lambda) \tilde{\gamma}^0 u(\tilde{\mathbf{p}}, \lambda) = 2\tilde{P}_z \quad (\text{A5b})$$

$$\bar{u}(\tilde{\mathbf{p}}', \lambda) \tilde{\gamma}_\perp^i u(\tilde{\mathbf{p}}, \lambda) = 2\tilde{P}_\perp^i - 2\lambda i\epsilon_{ij3} \tilde{\Delta}^j \quad (\text{A5c})$$

$$\bar{u}(\tilde{\mathbf{p}}', \lambda) \tilde{\gamma}^3 u(\tilde{\mathbf{p}}, \lambda) = 2\tilde{P}_z \left(1 - \frac{\tilde{E} + \tilde{E}'}{2\tilde{P}_z} \right) + \frac{2\lambda i(\tilde{\mathbf{P}}_\perp \times \tilde{\mathbf{\Delta}}_\perp) \cdot \hat{z}}{\tilde{P}_z}, \quad (\text{A5d})$$

where \tilde{E} and \tilde{E}' are the mass-shell energies of $\tilde{\mathbf{p}}$ and $\tilde{\mathbf{p}}'$, respectively. The gamma matrix elements in particular can be summarized in the following manifestly-covariant form:

$$\bar{u}(\tilde{\mathbf{p}}', \lambda) \tilde{\gamma}^\mu u(\tilde{\mathbf{p}}, \lambda) = 2\tilde{P}^\mu - \frac{2\lambda i\epsilon^{\mu\nu\rho\sigma} \tilde{n}_\nu \tilde{P}_\rho \tilde{\Delta}_\sigma}{(\tilde{\mathbf{P}} \cdot \tilde{\mathbf{n}})}, \quad (\text{A6})$$

where $\tilde{n}_\mu = (1; 0, 0, 0)$ projects out the “time” component of contravariant four-vectors (e.g., $\tilde{n}_\mu \tilde{x}^\mu = \tilde{x}^0 = \tilde{\tau}$).

Let us consider the helicity-flip case next. For $\lambda' \neq \lambda$, let $\Delta\lambda = \lambda' - \lambda$. We find:

$$\bar{u}(\tilde{\mathbf{p}}', \lambda') u(\tilde{\mathbf{p}}, \lambda) = (\Delta\lambda \tilde{\Delta}_x - i\tilde{\Delta}_y) \quad (\text{A7a})$$

$$\bar{u}(\tilde{\mathbf{p}}', \lambda') \tilde{\gamma}^0 u(\tilde{\mathbf{p}}, \lambda) = 0 \quad (\text{A7b})$$

$$\bar{u}(\tilde{\mathbf{p}}', \lambda') \tilde{\gamma}_\perp^i u(\tilde{\mathbf{p}}, \lambda) = 0 \quad (\text{A7c})$$

$$\bar{u}(\tilde{\mathbf{p}}', \lambda') \tilde{\gamma}^3 u(\tilde{\mathbf{p}}, \lambda) = -\frac{m}{\tilde{P}_z} (\Delta\lambda \tilde{\Delta}_x - i\tilde{\Delta}_y). \quad (\text{A7d})$$

Writing these in a manifestly-covariant manner is trickier, but can be done by utilizing the four-vector $\tilde{\mathbf{n}}^\mu = (1; 0, 0, 0)$ which projects out the “time” component of covariant four-vectors (e.g., $\tilde{n}^\mu \tilde{p}_\mu = \tilde{p}_0 = \tilde{E}$). Using Eq. (5), we note that $\tilde{n}^\mu = (0; 0, 0, -1)$ and $\tilde{\mathbf{n}}_\mu = (1; 0, 0, -1)$. With this in mind, we can write:

$$\bar{u}(\tilde{\mathbf{p}}', \lambda') u(\tilde{\mathbf{p}}, \lambda) = i\epsilon^{\alpha\beta\gamma\delta} \tilde{n}_\alpha \tilde{n}_\beta \tilde{\Delta}_\gamma (\sigma_\delta)_{\lambda'\lambda} \quad (\text{A8a})$$

$$\bar{u}(\tilde{\mathbf{p}}', \lambda') \tilde{\gamma}^\mu u(\tilde{\mathbf{p}}, \lambda) = \frac{m\tilde{n}^\mu}{(\tilde{\mathbf{P}} \cdot \tilde{\mathbf{n}})} i\epsilon^{\alpha\beta\gamma\delta} \tilde{n}_\alpha \tilde{n}_\beta \tilde{\Delta}_\gamma (\sigma_\delta)_{\lambda'\lambda} \quad (\text{A8b})$$

for $\lambda' \neq \lambda$, where $\sigma_\delta = (\mathbb{1}; \sigma_1, \sigma_2, \sigma_3)$ is a covariant four-vector of Pauli matrices.

The definite-helicity and helicity-flip cases can now be combined:

$$\bar{u}(\tilde{\mathbf{p}}', \lambda') u(\tilde{\mathbf{p}}, \lambda) = 2m(\sigma_0)_{\lambda'\lambda} + i\epsilon^{\alpha\beta\gamma\delta} \tilde{n}_\alpha \tilde{n}_\beta \tilde{\Delta}_\gamma (\sigma_\delta)_{\lambda'\lambda} \quad (\text{A9a})$$

$$\bar{u}(\tilde{\mathbf{p}}', \lambda') \tilde{\gamma}^\mu u(\tilde{\mathbf{p}}, \lambda) = 2\tilde{P}^\mu (\sigma_0)_{\lambda'\lambda} - \frac{i\epsilon^{\mu\nu\rho\sigma} \tilde{n}_\nu \tilde{P}_\rho \tilde{\Delta}_\sigma}{(\tilde{P} \cdot \tilde{n})} (\sigma_3)_{\lambda'\lambda} + \frac{m\tilde{n}^\mu}{(\tilde{P} \cdot \tilde{n})} i\epsilon^{\alpha\beta\gamma\delta} \tilde{n}_\alpha \tilde{n}_\beta \tilde{\Delta}_\gamma (\sigma_\delta)_{\lambda'\lambda}. \quad (\text{A9b})$$

Using Gordon decomposition, we can also write:

$$\bar{u}(\tilde{\mathbf{p}}', \lambda') \frac{i\sigma^{\mu\nu} \tilde{\Delta}_\nu}{2m} u(\tilde{\mathbf{p}}, \lambda) = -\frac{i\epsilon^{\mu\nu\rho\sigma} \tilde{n}_\nu \tilde{P}_\rho \tilde{\Delta}_\sigma}{(\tilde{P} \cdot \tilde{n})} (\sigma_3)_{\lambda'\lambda} + \left(\frac{m\tilde{n}^\mu}{(\tilde{P} \cdot \tilde{n})} - \frac{\tilde{P}^\mu}{m} \right) i\epsilon^{\alpha\beta\gamma\delta} \tilde{n}_\alpha \tilde{n}_\beta \tilde{\Delta}_\gamma (\sigma_\delta)_{\lambda'\lambda}. \quad (\text{A9c})$$

For the sake of explicit evaluations, it is helpful to note:

$$-\frac{i\epsilon^{0\nu\rho\sigma} \tilde{n}_\nu \tilde{P}_\rho \tilde{\Delta}_\sigma}{(\tilde{P} \cdot \tilde{n})} = 0 \quad (\text{A10a})$$

$$-\frac{i\epsilon^{i\nu\rho\sigma} \tilde{n}_\nu \tilde{P}_\rho \tilde{\Delta}_\sigma}{(\tilde{P} \cdot \tilde{n})} = i(\hat{z} \times \tilde{\Delta}_\perp)_i \quad : i = 1, 2 \quad (\text{A10b})$$

$$-\frac{i\epsilon^{3\nu\rho\sigma} \tilde{n}_\nu \tilde{P}_\rho \tilde{\Delta}_\sigma}{(\tilde{P} \cdot \tilde{n})} = \frac{i(\tilde{\mathbf{P}} \times \tilde{\Delta}_\perp) \cdot \hat{z}}{\tilde{P}_z} \quad (\text{A10c})$$

$$i\epsilon^{\alpha\beta\gamma\delta} \tilde{n}_\alpha \tilde{n}_\beta \tilde{\Delta}_\gamma (\sigma_\delta)_{\lambda'\lambda} = -i(\boldsymbol{\sigma}_{\lambda'\lambda} \times \tilde{\Delta}_\perp) \cdot \hat{z}. \quad (\text{A10d})$$

Appendix B: Uniqueness of light front synchronization

We prove two statements in this appendix. Firstly, for any coordinate system utilizing Cartesian spatial coordinates and a locally time-independent but otherwise arbitrary synchronization convention, it is impossible to express the physical electromagnetic current density of a spin-zero target as a three-dimensional internal density smeared by the probability current. In other words, there is no function $\rho(\mathbf{b})$ that is independent of the state $|\Psi\rangle$ such that:

$$\langle \Psi | \hat{j}^\mu(x) | \Psi \rangle = \int d^3\mathbf{R} \Psi^*(\mathbf{R}, t) i \overleftrightarrow{\partial}^\mu \Psi(\mathbf{R}, t) \rho(\mathbf{x} - \mathbf{R}) \quad (\text{B1})$$

for every state $|\Psi\rangle$. Secondly, the only possible coordinate systems which allow a two-dimensional reduction of the physical current density to be expressed as a two-dimensional internal density smeared by the probability current is a tilted light front coordinate system with an arbitrary unit vector \mathbf{n} defining the longitudinal direction.

One clarification is in order before proceeding. We mean that a time synchronization convention is locally time-independent if the proper time element $d\tau = \sqrt{g_{\mu\nu} dx^\mu dx^\nu}$ measured by a stationary clock at any location is always dt . This means we must have $\tilde{g}_{00} = 1$ in the transformed coordinate system. In other words, we choose *by convention* [25] that the local time coordinate should match the physical time measured by a local stationary clock.

The coordinate system for the hypothetical time synchronization convention can be written:

$$\tilde{x}^0 = x^0 + S(x) \quad (\text{B2a})$$

$$\tilde{x}^1 = x^1 \quad (\text{B2b})$$

$$\tilde{x}^2 = x^2 \quad (\text{B2c})$$

$$\tilde{x}^3 = x^3, \quad (\text{B2d})$$

where we use tildes for the transformed coordinates, and where we call $S(x)$ the synchronization function. The requirement of local time independence imposes:

$$\tilde{g}_{00} = \frac{\partial x^\mu}{\partial \tilde{x}^0} \frac{\partial x^\nu}{\partial \tilde{x}^0} g_{\mu\nu} = \left(1 + \frac{\partial S(x)}{\partial x^0} \right)^2 = 1, \quad (\text{B3})$$

and thus:

$$S(x) = S(\mathbf{x}). \quad (\text{B4})$$

The synchronization function is therefore a function only of space.

1. The non-existence of three-dimensional densities

To proceed, require an expression for the physical density $\langle \Psi | \hat{j}^\mu(\tilde{x}) | \Psi \rangle$ in terms of the transformed coordinates. To avoid any complications related to trying to quantize the theory on a curvilinear equal-time surface, we proceed within instant form quantization and Minkowski coordinates, and obtain a formula to which the coordinates can be transformed according to Eq. (B2) directly.

Since matrix elements for momentum kets can be written:

$$\langle \mathbf{p}' | \hat{j}^\mu(0) | \mathbf{p} \rangle = 2P^\mu F(\Delta^2), \quad (\text{B5})$$

the physical electromagnetic four-current density is:

$$\langle j^\mu(x) \rangle \equiv \langle \Psi | \hat{j}^\mu(x) | \Psi \rangle = \int \frac{d^3\mathbf{p}}{2E_{\mathbf{p}}(2\pi)^3} \int \frac{d^3\mathbf{p}'}{2E_{\mathbf{p}'}(2\pi)^3} \langle \Psi | \mathbf{p}' \rangle e^{ip' \cdot x} 2P^\mu F(\Delta^2) \langle \mathbf{p} | \Psi \rangle e^{-ip \cdot x}. \quad (\text{B6})$$

Similar to the procedure in Sec. IV A, one can substitute $2P^\mu \mapsto i \overleftrightarrow{\partial}^\mu$ here. Additionally, the substitution

$$\Delta \mapsto -i(\overrightarrow{\partial} + \overleftarrow{\partial})$$

can be made. If this substitution is formally made within the form factor, we obtain:

$$\langle j^\mu(x) \rangle = F(-\partial^2) \left[\left(\int \frac{d^3\mathbf{p}'}{2E_{\mathbf{p}'}(2\pi)^3} \langle \Psi | \mathbf{p}' \rangle e^{ip' \cdot x} \right) i \overleftrightarrow{\partial}^\mu \left(\int \frac{d^3\mathbf{p}}{2E_{\mathbf{p}}(2\pi)^3} \langle \mathbf{p} | \Psi \rangle e^{-ip \cdot x} \right) \right]. \quad (\text{B7})$$

The position-representation wave function can be defined in a covariant way in terms of the field operator $\hat{\phi}(x)$:

$$\Psi(\mathbf{x}, t) = \langle 0 | \hat{\phi}(x) | \Psi \rangle, \quad (\text{B8})$$

which is related to the momentum-representation wave function by:

$$\Psi(\mathbf{x}, t) = \int \frac{d^3\mathbf{p}}{2E_{\mathbf{p}}(2\pi)^3} \langle \mathbf{p} | \Psi \rangle e^{-ip \cdot x}. \quad (\text{B9})$$

Thus, the physical electromagnetic current density can be written:

$$\langle j^\mu(x) \rangle = F(-\partial^2) \left[\Psi^*(\mathbf{x}, t) i \overleftrightarrow{\partial}^\mu \Psi(\mathbf{x}, t) \right] \equiv F(-\partial^2) \mathcal{J}^\mu(x). \quad (\text{B10})$$

Each piece of this expression can be rewritten in terms of the alternative coordinate system by employing Eq. (B2):

$$\langle \tilde{j}^\mu(\tilde{x}) \rangle = F(-\tilde{\partial}^2) \left[\Psi^*(\tilde{\mathbf{x}}, \tilde{\tau}) i \overleftrightarrow{\partial}^\mu \Psi(\tilde{\mathbf{x}}, \tilde{\tau}) \right] \equiv F(-\tilde{\partial}^2) \tilde{\mathcal{J}}^\mu(\tilde{x}). \quad (\text{B11})$$

To proceed, we need the d'Alembertian in the transformed coordinate system. In a general coordinate system [47]:

$$\tilde{\partial}^2 f(\tilde{x}) = \frac{1}{\sqrt{-\tilde{g}}} \tilde{\partial}_\mu \left[\sqrt{-\tilde{g}} \tilde{g}^{\mu\nu} \tilde{\partial}_\nu f(\tilde{x}) \right], \quad (\text{B12})$$

where $\tilde{g} = \det(\tilde{g}_{\mu\nu})$. The inverse metric in this coordinate system is:

$$\tilde{g}^{\mu\nu} = \frac{\partial \tilde{x}^\mu}{\partial x^\alpha} \frac{\partial \tilde{x}^\nu}{\partial x^\beta} g^{\alpha\beta} = \begin{bmatrix} 1 - (\nabla S)^2 & -\nabla_x S & -\nabla_y S & -\nabla_z S \\ -\nabla_x S & -1 & 0 & 0 \\ -\nabla_y S & 0 & -1 & 0 \\ -\nabla_z S & 0 & 0 & -1 \end{bmatrix}, \quad (\text{B13})$$

and its determinant is -1 , meaning the determinant of $\tilde{g}_{\mu\nu}$ is also -1 . Thus, the d'Alembertian in the transformed coordinates can be written:

$$\tilde{\partial}^2 = (1 - (\nabla S)^2) \tilde{\partial}_0^2 - (\nabla^2 S) \tilde{\partial}_0 - (\nabla S) \cdot \tilde{\nabla} \tilde{\partial}_0 - \tilde{\nabla}^2. \quad (\text{B14})$$

If a three-dimensional state-independent electric charge density exists, then the following relation should be satisfied for any state $|\Psi\rangle$:

$$\langle \tilde{j}^\mu(\tilde{x}) \rangle = \int d^3\tilde{\mathbf{R}} \tilde{\mathcal{P}}^\mu(\tilde{\mathbf{R}}, \tilde{\tau}) \rho(\tilde{\mathbf{x}} - \tilde{\mathbf{R}}). \quad (\text{B15})$$

Using Eqs. (B11) and (B14), this means:

$$F\left(-\left(1 - (\nabla S)^2\right)\tilde{\partial}_0^2 + (\nabla^2 S)\tilde{\partial}_0 + (\nabla S) \cdot \tilde{\nabla}\tilde{\partial}_0 + \tilde{\nabla}^2\right)\tilde{\mathcal{P}}^\mu(\tilde{x}) = \int d^3\tilde{\mathbf{R}} \tilde{\mathcal{P}}^\mu(\tilde{\mathbf{R}}, \tilde{\tau}) \rho(\tilde{\mathbf{x}} - \tilde{\mathbf{R}}). \quad (\text{B16})$$

By introducing $\varphi(\mathbf{k})$ as the Fourier transform of the charge density:

$$\rho(\tilde{\mathbf{b}}) = \int \frac{d^3\mathbf{k}}{(2\pi)^3} \varphi(\mathbf{k}) e^{-i\mathbf{k} \cdot \tilde{\mathbf{b}}}, \quad (\text{B17})$$

it follows that:

$$\int d^3\tilde{\mathbf{R}} \tilde{\mathcal{P}}^\mu(\tilde{\mathbf{R}}, \tilde{\tau}) \rho(\tilde{\mathbf{x}} - \tilde{\mathbf{R}}) = \varphi(i\tilde{\nabla}) \tilde{\mathcal{P}}^\mu(\tilde{\mathbf{x}}, \tilde{\tau}), \quad (\text{B18})$$

and Eq. (B16) becomes:

$$F\left(-\left(1 - (\nabla S)^2\right)\tilde{\partial}_0^2 + (\nabla^2 S)\tilde{\partial}_0 + (\nabla S) \cdot \tilde{\nabla}\tilde{\partial}_0 + \tilde{\nabla}^2\right)\tilde{\mathcal{P}}^\mu(\tilde{x}) = \varphi(i\tilde{\nabla}) \tilde{\mathcal{P}}^\mu(\tilde{\mathbf{x}}, \tilde{\tau}). \quad (\text{B19})$$

The requirement that this holds for any state imposes:

$$F\left(-\left(1 - (\nabla S)^2\right)\tilde{\partial}_0^2 + (\nabla^2 S)\tilde{\partial}_0 + (\nabla S) \cdot \tilde{\nabla}\tilde{\partial}_0 + \tilde{\nabla}^2\right) = \varphi(i\tilde{\nabla}), \quad (\text{B20})$$

in which the right-hand side depends only on spatial derivatives. This equality can only hold if the left-hand side does not depend on $\tilde{\partial}_0$, which imposes the following three constraints that cannot simultaneously hold:

$$\nabla^2 S = 0 \quad (\text{B21a})$$

$$(\nabla S)^2 = 1 \quad (\text{B21b})$$

$$\nabla S = 0. \quad (\text{B21c})$$

In particular, the second and third conditions contradict each other. We therefore conclude that no state-independent three-dimensional internal charge density exists, regardless of the synchronization convention used.

2. The uniqueness of light front synchronization

Although no three-dimensional internal density exists, we already know that light front synchronization allows an internal two-dimensional density to be found. We next inquire whether other synchronization conventions permit alternative two-dimensional densities to be obtained. (For instance, is there a synchronization convention that is rotationally symmetric and allows an angular density to be obtained by integrating out the radial coordinate?)

In the formulation used in this appendix, light front synchronization works by eliminating derivatives with respect to the spatial coordinate that has been integrated out. Thus, the term $(\nabla S) \cdot \tilde{\nabla}\tilde{\partial}_0$ in the d'Alembertian can be made to vanish without requiring that $\nabla S = 0$. The way that works with $S(\mathbf{x}) = z$ as an example is:

$$\begin{aligned} \int_{-\infty}^{\infty} d\tilde{z} F\left(\tilde{\partial}_z\tilde{\partial}_0 + \tilde{\nabla}^2\right)\tilde{\mathcal{P}}^\mu(\tilde{x}) &= \sum_{n=0}^{\infty} \frac{F^{(n)}(0)}{n!} \int_{-\infty}^{\infty} d\tilde{z} \left(\tilde{\partial}_z\tilde{\partial}_0 + \tilde{\nabla}^2\right)^n \tilde{\mathcal{P}}^\mu(\tilde{x}) \\ &= \sum_{n=0}^{\infty} \sum_{k=0}^n \frac{F^{(n)}(0)}{n!} \int_{-\infty}^{\infty} d\tilde{z} \tilde{\partial}_z^{n-k} \tilde{\partial}_0^{n-k} (\tilde{\nabla}^2)^k \tilde{\mathcal{P}}^\mu(\tilde{x}) \\ &= \sum_{n=0}^{\infty} \frac{F^{(n)}(0)}{n!} \int_{-\infty}^{\infty} d\tilde{z} (\tilde{\nabla}^2)^n \tilde{\mathcal{P}}^\mu(\tilde{x}) = \int_{-\infty}^{\infty} d\tilde{z} F(\tilde{\nabla}^2) \tilde{\mathcal{P}}^\mu(\tilde{x}). \end{aligned} \quad (\text{B22})$$

Thus, to obtain two-dimensional densities, only the first two conditions of Eq. (B21) are required to hold.

The most general solution to $\nabla^2 S = 0$ without a singularity at the origin is:

$$S(\mathbf{r}) = \sum_{l=0}^{\infty} r^l \sum_{m=-l}^l C_{lm} Y_{lm}(\theta, \phi). \quad (\text{B23})$$

For this general solution:

$$(\nabla S)^2 = \sum_{l,l'} r^{l+l'-2} \sum_{m=-l}^l \sum_{m'=-l'}^{l'} C_{lm} C_{l'm'}^* \left(ll' Y_{lm}(\theta, \phi) Y_{l'm'}^*(\theta, \phi) + \frac{\partial Y_{lm}(\theta, \phi)}{\partial \theta} \frac{\partial Y_{l'm'}^*(\theta, \phi)}{\partial \theta} + \frac{1}{\sin^2 \theta} \frac{\partial Y_{lm}(\theta, \phi)}{\partial \phi} \frac{\partial Y_{l'm'}^*(\theta, \phi)}{\partial \phi} \right). \quad (\text{B24})$$

To obtain $(\nabla S)^2 = 1$, it is necessary that every power of r greater than 0 vanish in this expression. Thus, for any $n > 0$:

$$\sum_{l=0}^{n+2} \sum_{l'=0}^{n+2} \delta_{l',n+2-l} \sum_{m=-l}^l \sum_{m'=-l'}^{l'} C_{lm} C_{l'm'}^* \left(ll' Y_{lm}(\theta, \phi) Y_{l'm'}^*(\theta, \phi) + \frac{\partial Y_{lm}(\theta, \phi)}{\partial \theta} \frac{\partial Y_{l'm'}^*(\theta, \phi)}{\partial \theta} + \frac{1}{\sin^2 \theta} \frac{\partial Y_{lm}(\theta, \phi)}{\partial \phi} \frac{\partial Y_{l'm'}^*(\theta, \phi)}{\partial \phi} \right) = 0. \quad (\text{B25})$$

Integrating this over the surface of a unit sphere, and using integration by parts, gives:

$$\sum_{l=0}^{n+2} \sum_{l'=0}^{n+2} \delta_{l',n+2-l} \sum_{m=-l}^l \sum_{m'=-l'}^{l'} C_{lm} C_{l'm'}^* \int_0^\pi d\theta \sin \theta \int_0^{2\pi} d\phi Y_{l'm'}^*(\theta, \phi) \left(ll' Y_{lm}(\theta, \phi) + \frac{1}{\sin \theta} \frac{\partial}{\partial \theta} \left[\sin \theta \frac{\partial Y_{lm}(\theta, \phi)}{\partial \theta} \right] - \frac{1}{\sin^2 \theta} \frac{\partial^2 Y_{lm}(\theta, \phi)}{\partial \phi^2} \right) = 0. \quad (\text{B26})$$

Using the differential equation defining the spherical harmonics, and their orthogonality, gives:

$$\sum_{l=0}^{n+2} \sum_{l'=0}^{n+2} \delta_{l',n+2-l} \sum_{m=-l}^l \sum_{m'=-l'}^{l'} C_{lm} C_{l'm'}^* \delta_{ll'} \delta_{mm'} l(l' + l + 1) = 0. \quad (\text{B27})$$

The Kronecker delta product $\delta_{l',n+2-l} \delta_{ll'}$ will give 0 automatically if n is odd. For even n , using the Kronecker deltas to eliminate most the sums gives:

$$\sum_{m=-l}^l |C_{lm}|^2 \Big|_{l=n/2+1} = 0. \quad (\text{B28})$$

Since this must be true for even $n > 0$, it must be true for any $l > 1$. Thus $C_{lm} = 0$ for all $l > 1$. The most general possible S satisfying the first two conditions of Eq. (B21) is thus:

$$S(\mathbf{r}) = S_0 + \mathbf{n} \cdot \mathbf{r}, \quad (\text{B29})$$

with S_0 a constant and $\mathbf{n}^2 = 1$. Here S_0 is simply a global time offset. This most general possible solution defines light front synchronization, with \mathbf{n} defining the longitudinal direction. Therefore, light front synchronization is the only synchronization convention that allows an internal two-dimensional density to be defined.

-
- [1] Maxim V. Polyakov and Peter Schweitzer, “Forces inside hadrons: pressure, surface tension, mechanical radius, and all that,” *Int. J. Mod. Phys. A* **33**, 1830025 (2018), [arXiv:1805.06596 \[hep-ph\]](#).
[2] Cédric Lorcé, Hervé Moutarde, and Arkadiusz P. Trawiński, “Revisiting the mechanical properties of the nucleon,” *Eur. Phys. J. C* **79**, 89 (2019), [arXiv:1810.09837 \[hep-ph\]](#).
[3] Adam Freese and Gerald A. Miller, “Forces within hadrons on the light front,” *Phys. Rev. D* **103**, 094023 (2021), [arXiv:2102.01683 \[hep-ph\]](#).

- [4] J. Yu. Panteleeva, E. Epelbaum, J. Gegelia, and U. G. Meißner, “Definition of gravitational local spatial densities for spin-0 and spin-1/2 systems,” (2022), [arXiv:2211.09596 \[hep-ph\]](#).
- [5] Daniel Boer *et al.*, “Gluons and the quark sea at high energies: Distributions, polarization, tomography,” (2011), [arXiv:1108.1713 \[nucl-th\]](#).
- [6] A. Accardi *et al.*, “Electron Ion Collider: The Next QCD Frontier: Understanding the glue that binds us all,” *Eur. Phys. J. A* **52**, 268 (2016), [arXiv:1212.1701 \[nucl-ex\]](#).
- [7] R. Abdul Khalek *et al.*, “Science Requirements and Detector Concepts for the Electron-Ion Collider: EIC Yellow Report,” (2021), [arXiv:2103.05419 \[physics.ins-det\]](#).
- [8] R.G. Sachs, “High-Energy Behavior of Nucleon Electromagnetic Form Factors,” *Phys. Rev.* **126**, 2256–2260 (1962).
- [9] Gordon N. Fleming, “Charge Distributions from Relativistic Form-Factors,” in *Physical reality and mathematical description: Festschrift Jauch (Josef Maria) on his 60th birthday*, edited by Charles P. Enz and Jagdish Mehra (1974) pp. 357–374.
- [10] Matthias Burkardt, “Impact parameter dependent parton distributions and off forward parton distributions for $\zeta \rightarrow 0$,” *Phys. Rev. D* **62**, 071503 (2000), [Erratum: *Phys.Rev.D* 66, 119903 (2002)], [arXiv:hep-ph/0005108](#).
- [11] Gerald A. Miller, “Defining the proton radius: A unified treatment,” *Phys. Rev. C* **99**, 035202 (2019), [arXiv:1812.02714 \[nucl-th\]](#).
- [12] E. Epelbaum, J. Gegelia, N. Lange, U. G. Meißner, and M. V. Polyakov, “Definition of Local Spatial Densities in Hadrons,” *Phys. Rev. Lett.* **129**, 012001 (2022), [arXiv:2201.02565 \[hep-ph\]](#).
- [13] Yang Li, Wen-bo Dong, Yi-liang Yin, Qun Wang, and James P. Vary, “Minkowski’s lost legacy and hadron electromagnetism,” *Phys. Lett. B* **838**, 137676 (2023), [arXiv:2206.12903 \[hep-ph\]](#).
- [14] Yi Chen and Cédric Lorcé, “Pion and nucleon relativistic electromagnetic four-current distributions,” *Phys. Rev. D* **106**, 116024 (2022), [arXiv:2210.02908 \[hep-ph\]](#).
- [15] Adam Freese and Gerald A. Miller, “On the true meaning of spatial densities of hadrons,” (2022), [arXiv:2210.03807 \[hep-ph\]](#).
- [16] Matthias Burkardt, “Impact parameter space interpretation for generalized parton distributions,” *Int. J. Mod. Phys. A* **18**, 173–208 (2003), [arXiv:hep-ph/0207047](#).
- [17] Gerald A. Miller, “Transverse Charge Densities,” *Ann. Rev. Nucl. Part. Sci.* **60**, 1–25 (2010), [arXiv:1002.0355 \[nucl-th\]](#).
- [18] M. Diehl, “Generalized parton distributions in impact parameter space,” *Eur. Phys. J. C* **25**, 223–232 (2002), [Erratum: *Eur.Phys.J.C* 31, 277–278 (2003)], [arXiv:hep-ph/0205208](#).
- [19] Xiang-Dong Ji, “Off forward parton distributions,” *J. Phys. G* **24**, 1181–1205 (1998), [arXiv:hep-ph/9807358](#).
- [20] M. Diehl, “Generalized parton distributions,” *Phys. Rept.* **388**, 41–277 (2003), [arXiv:hep-ph/0307382 \[hep-ph\]](#).
- [21] P. G. Blunden, M. Burkardt, and G. A. Miller, “Light front nuclear physics: Toy models, static sources and tilted light front coordinates,” *Phys. Rev. C* **61**, 025206 (2000), [arXiv:nucl-th/9908067](#).
- [22] Albert Einstein, “On the electrodynamics of moving bodies,” *Annalen Phys.* **17**, 891–921 (1905).
- [23] Yuan Zhong Zhang, “Test theories of special relativity,” *General Relativity and Gravitation* **27**, 475–493 (1995).
- [24] Ronald Anderson, Geoffrey E. Stedman, and I. Vetharaniam, “Conventionality of synchronisation, gauge dependence and test theories of relativity,” *Phys. Rept.* **295**, 93–180 (1998).
- [25] H. Reichenbach, *The Philosophy of Space and Time*, Dover Books on Physics (Dover Publications, 2012).
- [26] A. Grünbaum, *Philosophical Problems of Space and Time: Second, enlarged edition*, Boston Studies in the Philosophy and History of Science (Springer Netherlands, 2012).
- [27] Derek Muller and Petr Lebedev, “Why No One Has Measured The Speed Of Light,” (2020).
- [28] D. E. Soper, “Infinite-momentum helicity states,” *Phys. Rev. D* **5**, 1956–1962 (1972).
- [29] Cédric Lorcé, Andreas Metz, Barbara Pasquini, and Simone Rodini, “Energy-momentum tensor in QCD: nucleon mass decomposition and mechanical equilibrium,” *JHEP* **11**, 121 (2021), [arXiv:2109.11785 \[hep-ph\]](#).
- [30] Roger Penrose, “The Apparent shape of a relativistically moving sphere,” *Proc. Cambridge Phil. Soc.* **55**, 137–139 (1959).
- [31] James Terrell, “Invisibility of the Lorentz Contraction,” *Phys. Rev.* **116**, 1041–1045 (1959).
- [32] V. Bargmann, “On Unitary ray representations of continuous groups,” *Annals Math.* **59**, 1–46 (1954).
- [33] G Pinski, “Galilean tensor calculus,” *Journal of Mathematical Physics* **9**, 1927–1930 (1968).
- [34] Y. Takahashi, “Towards the Many Body Theory With the Galilei Invariance as a Guide. 1,” *Fortsch. Phys.* **36**, 63–81 (1988).
- [35] JK Lubanski, “Sur la theorie des particules élémentaires de spin quelconque. i,” *Physica* **9**, 310–324 (1942).
- [36] JK Lubanski, “Sur la théorie des particules élémentaires de spin quelconque. ii,” *Physica* **9**, 325–338 (1942).
- [37] Carl E. Carlson and Marc Vanderhaeghen, “Empirical transverse charge densities in the nucleon and the nucleon-to-Delta transition,” *Phys. Rev. Lett.* **100**, 032004 (2008), [arXiv:0710.0835 \[hep-ph\]](#).
- [38] Gerald A. Miller, “Charge Density of the Neutron,” *Phys. Rev. Lett.* **99**, 112001 (2007), [arXiv:0705.2409 \[nucl-th\]](#).
- [39] Gerald A. Miller, “Electromagnetic Form Factors and Charge Densities From Hadrons to Nuclei,” *Phys. Rev. C* **80**, 045210 (2009), [arXiv:0908.1535 \[nucl-th\]](#).
- [40] J. J. Kelly, “Simple parametrization of nucleon form factors,” *Phys. Rev. C* **70**, 068202 (2004).
- [41] S. Riordan *et al.*, “Measurements of the Electric Form Factor of the Neutron up to $Q^2 = 3.4 \text{ GeV}^2$ using the Reaction $^3\text{He} \rightarrow (e^-, e'n)pp$,” *Phys. Rev. Lett.* **105**, 262302 (2010), [arXiv:1008.1738 \[nucl-ex\]](#).
- [42] Anthony W. Thomas, “Interplay of Spin and Orbital Angular Momentum in the Proton,” *Phys. Rev. Lett.* **101**, 102003 (2008), [arXiv:0803.2775 \[hep-ph\]](#).
- [43] Adam Freese and Ian C. Cloët, “Quark spin and orbital angular momentum from proton generalized parton distributions,” *Phys. Rev. C* **103**, 045204 (2021), [arXiv:2005.10286 \[nucl-th\]](#).
- [44] C. Alexandrou, M. Constantinou, K. Hadjiyiannakou, K. Jansen, C. Kallidonis, G. Koutsou, A. Vaquero Avilés-Casco, and C. Wiese, “Nucleon Spin and Momentum Decomposition Using Lattice QCD Simulations,” *Phys. Rev. Lett.* **119**, 142002 (2017), [arXiv:1706.02973 \[hep-lat\]](#).
- [45] E. Leader and C. Lorcé, “The angular momentum controversy: What’s it all about and does it matter?” *Phys. Rept.* **541**, 163–248 (2014),

[arXiv:1309.4235 \[hep-ph\]](#).

- [46] John B. Kogut and Davison E. Soper, “Quantum Electrodynamics in the Infinite Momentum Frame,” [Phys. Rev. D **1**, 2901–2913 \(1970\)](#).
- [47] M. Nakahara, [Geometry, Topology and Physics, Second Edition](#), Graduate student series in physics (Taylor & Francis, 2003).